

MARCH 31, 2023
Revision 1: July 20, 2023



Native Villages, Alaska 2022 Lidar Technical Data Report

Task Order: 140G0222F0194

Project ID: 230374

Prepared For:



USGS

1400 Independence Road
Rolla, MO 65401

Contract: 140G0221D0012

Work Unit ID: 300198 - 300201

Prepared By:



NV5 Geospatial Anchorage Office

2014 Merrill Field Drive
Anchorage, AK 99501
PH: 907-272-4495

TABLE OF CONTENTS

INTRODUCTION	8
Deliverable Products	10
ACQUISITION	12
Planning	12
Airborne Lidar Survey	13
Ground Survey	16
Base Stations	16
Ground Survey Points (GSPs)	17
Land Cover Class	17
PROCESSING	19
NIR Lidar Data	19
Feature Extraction	22
Hydroflattening and Water’s Edge Breaklines	22
Hydro-Flattened Raster DEM Processing	22
Roads	24
Intensity Image Processing	24
Swath Separation Raster Processing	25
Maximum Surface Height Raster Processing	25
RESULTS & DISCUSSION	26
Lidar Density	26
Lidar Accuracy Assessments	34
Lidar Non-Vegetated Vertical Accuracy	34
Lidar Vegetated Vertical Accuracies	42
Lidar Relative Vertical Accuracy	47
Lidar Horizontal Accuracy	50
CERTIFICATIONS	51
GLOSSARY	52
APPENDIX A - ACCURACY CONTROLS	1

Cover Photo: A view looking at the Tuntuliak village in the Native Villages project. The image was created from the lidar bare earth model overlaid with the above ground point cloud and virtual earth imagery and colored by elevation.

LIST OF FIGURES

Figure 1: Location map of the Native Villages site in Alaska	11
Figure 2: Flightlines map for projection zones 3 and 4.....	14
Figure 3: Flightlines map for projection zones 5 and 6.....	15
Figure 4: Ground survey location map.....	18
Figure 5: Example of hydroflattening in the Native Villages Lidar dataset.....	23
Figure 6: Sample Image of road surface lidar classified points (orange lines) within the Native Villages boundary.....	24
Figure 7: The color ramp values used in the Native Villages project.....	25
Figure 8: Frequency distribution of first return point density values per 100 x 100 m cell for UTM 3.....	28
Figure 9: Frequency distribution of ground-classified return point density values per 100 x 100 m cell for UTM 3.....	28
Figure 10: Frequency distribution of ground-classified return point density values per 100 x 100 m cell for UTM 4.....	29
Figure 11: Frequency distribution of ground-classified return point density values per 100 x 100 m cell for UTM 4.....	29
Figure 12: Frequency distribution of ground-classified return point density values per 100 x 100 m cell for UTM 5.....	30
Figure 13: Frequency distribution of ground-classified return point density values per 100 x 100 m cell for UTM 5.....	30
Figure 14: Frequency distribution of ground-classified return point density values per 100 x 100 m cell for UTM 6.....	31
Figure 15: Frequency distribution of ground-classified return point density values per 100 x 100 m cell for UTM 6.....	31
Figure 16: First return point density map for the Native Villages sites (100 m x 100 m cells).....	32
Figure 17: Ground classified point density map for the Native Villages sites (100 m x 100 m cells).....	33
Figure 18: Frequency histogram for the lidar classified LAS deviation from ground check point values (NVA) for the zone UTM 3.....	36
Figure 19: Frequency histogram for the lidar bare earth DEM surface deviation from ground check point values (NVA) for the zone UTM 3.....	36
Figure 20: Frequency histogram for the lidar surface deviation from ground control point values for the zone UTM 3.....	37
Figure 21: Frequency histogram for the lidar classified LAS deviation from ground check point values (NVA) for the zone UTM 4.....	37
Figure 22: Frequency histogram for the lidar bare earth DEM surface deviation from ground check point values (NVA) for the zone UTM 4.....	38
Figure 23: Frequency histogram for the lidar surface deviation from ground control point values for the zone UTM 4.....	38
Figure 24: Frequency histogram for the lidar classified LAS deviation from ground check point values (NVA) for the zone UTM 5.....	39
Figure 25: Frequency histogram for the lidar bare earth DEM surface deviation from ground check point values (NVA) for the zone UTM 5.....	39
Figure 26: Frequency histogram for the lidar surface deviation from ground control point values for the zone UTM 5.....	40

Figure 27: Frequency histogram for the lidar classified LAS deviation from ground check point values (NVA) for the zone UTM 6.....	40
Figure 28: Frequency histogram for the lidar bare earth DEM surface deviation from ground check point values (NVA) for the zone UTM 6	41
Figure 29: Frequency histogram for the lidar surface deviation from ground control point values for the zone UTM 6	41
Figure 30: Frequency histogram for the lidar surface deviation from all land cover class point values (VVA) for the zone UTM 3	43
Figure 31: Frequency histogram for the lidar bare earth DEM deviation from vegetated check point values (VVA) for the zone UTM 3.....	43
Figure 32: Frequency histogram for the lidar surface deviation from all land cover class point values (VVA) for the zone UTM 4	44
Figure 33: Frequency histogram for the lidar bare earth DEM deviation from vegetated check point values (VVA) for the zone UTM 4.....	44
Figure 34: Frequency histogram for the lidar surface deviation from all land cover class point values (VVA) for the zone UTM 5	45
Figure 35: Frequency histogram for the lidar bare earth DEM deviation from vegetated check point values (VVA) for the zone UTM 5.....	45
Figure 36: Frequency histogram for the lidar surface deviation from all land cover class point values (VVA) for the zone UTM 6	46
Figure 37: Frequency histogram for the lidar bare earth DEM deviation from vegetated check point values (VVA) for the zone UTM 6.....	46
Figure 38: Frequency plot for the relative vertical accuracy between flight lines for UTM 3	48
Figure 39: Frequency plot for the relative vertical accuracy between flight lines for UTM 4	48
Figure 40: Frequency plot for the relative vertical accuracy between flight lines for UTM 5	49
Figure 41: Frequency plot for the relative vertical accuracy between flight lines for UTM 6	49

LIST OF TABLES

Table 1: Acquisition dates, acreage, and data types collected on the Native Villages site in Alaska	9
Table 2: Deliverable product projection information	10
Table 3: Products delivered to USGS for the Native Villages sites.....	10
Table 4: Flight Date Table	12
Table 5: Lidar specifications and survey settings.....	13
Table 6: Base station positions for the Native Villages acquisition. Coordinates are on the NAD83 (2011) datum, epoch 2010.00	16
Table 7: Land Cover Types and Descriptions	17
Table 8: Software used for statistical analysis	20
Table 9: Lidar processing workflow	20
Table 10: ASPRS LAS classification standards applied to the Native Villages dataset.....	21
Table 11: Average lidar point densities.....	27
Table 12: Absolute accuracy results	35
Table 13: Vegetated vertical accuracy results	42
Table 14: Relative accuracy results.....	47
Table 15: Horizontal Accuracy	50

INTRODUCTION

This photo, taken by DOWL, shows a view of the Shaktoolik village in the Native Villages site in Alaska.



In July 2022, NV5 Geospatial (NV5) was contracted by the United States Geologic Survey (USGS) to collect Light Detection and Ranging (lidar) data in the fall of 2022 during leaf-off conditions for the Native Villages sites in Alaska. The full area of interest (AOI) includes 14 AOIs of varying size and isolation located outside of villages that are spread throughout Alaska. This report and associated data set covers 9 out of the 14 AOIs. The list of the areas pertaining to this report can be found in Table 1. The 9 AOIs span across four UTM zones and four regions, or native corporations.

Alaska was divided into twelve geographic and cultural regions, where the people share interests and a common heritage, as per the Alaska Native Claims Settlement Act (ANCSA) of 1971. Each of these village corporations are owned by Alaska Native shareholders. The village corporations in this project are the Bering Straits, Calista, Doyon, and Cook Inlet. The Bering Straits Native Corporation encompasses most of the Seaward Peninsula, eastern coast of the Norton Sound, and some coastline along the Bering Sea and Chukchi Sea. The Calista region, directly south of the Bering Straits region, is very remote and not accessible by roads. Like the Bering Straits region, it includes part of the Bering Sea coastline that stretches to the mouth of the lower Yukon River. The Cook's Inlet region is east of the Calista region in south-central Alaska and includes the city of Anchorage. The last native corporation acquired in this project is the Doyon Native Corporation, which makes up a large portion of the central Alaskan mainland and includes the city of Fairbanks.

Data were collected to aid the USGS and National Resources and Conservation Service (NRCS) in assessing the topographic and geophysical properties of the study area to support the 3DEP mission. The USGS 3DEP mission is to obtain elevation data to better manage and protect lives, property, and the environment as well as improve planning for future projects. Specifically, the AOIs are being assessed as higher ground alternatives for the adjacent villages since the sea level is predicted to rise significantly in these areas, due to climate change and the melting of sea ice, over the next 30 years.

This report accompanies the delivered lidar data, and documents contract specifications, data acquisition procedures, processing methods, and analysis of the final dataset including lidar accuracy and density. Acquisition dates and acreage are shown in Table 1, deliverable projection information is shown in Table 2, a complete list of contracted deliverables provided to USGS is shown in Table 3, and the project extent is shown in Figure 1.

Table 1: Acquisition dates, acreage, and data types collected on the Native Villages site in Alaska

Project Site	Native Corp./Region	UTM Zone	Contracted Acres	Contracted Sq. Miles	Acquisition Dates	Data Type
Golovin	Bering Straits	3	6,983	10.91	10/14/2022	NIR - Lidar
Atmautluak	Calista	3	36,112	56.42	8/11/2022	NIR - Lidar
Tuntutuliak	Calista	3	10,134	15.84	8/11/2022	NIR - Lidar
Kwigillingok	Calista	3	7,648	11.95	8/11/2022	NIR - Lidar
Akiak	Calista	4	10,992	17.18	8/11/2022	NIR - Lidar
Shaktoolik	Bering Straits	4	24,703	38.60	10/14/2022	NIR - Lidar
McGrath	Doyon	5	19,935	31.15	8/10/2022	NIR - Lidar
Tyonek	Cook Inlet	5	53,465	83.54	10/21/2022	NIR - Lidar
Fort Yukon	Doyon	6	16,090	25.14	8/13/2022	NIR - Lidar
Total	All	3 - 6	186,062	290.73	8/10/2022 - 10/21/2022	NIR - Lidar

Deliverable Products

Table 2: Deliverable product projection information

Projections	Horizontal Datum	Vertical Datum	Units
UTM Zone 3 through 6	NAD83 (2011)	NAVD88 (GEOID12b)	Meters

Table 3: Products delivered to USGS for the Native Villages sites

Product Type	File Type	Product Details
Points	LAS v.1.4 (*.las)	All Classified Returns
Rasters	1.0 meter Cloud-Optimized GeoTIFFs	Hydroflattened Bare Earth Digital Elevation Model (DEM) Maximum Surface Height Raster (MSHR) Swath Separation Rasters Intensity Images
Vectors	Shapefiles (*.shp)	Defined Project Area (DPA) Master Tile Index (MTI) Road Planimetrics
Vectors	ESRI File Geodatabase (*.gdb)	Flightline Index Flightline Swaths 3D Water's Edge Breaklines 3D Bridge Breaklines
Vectors	QGIS Geopackage (*.gpkg)	Ground Survey Shapes
Metadata	Extensible Markup Language (*.xml)	Metadata
Reports	Adobe Acrobat (*.pdf)	Ground Survey Report Lidar Technical Data Report SBET Quality Reports

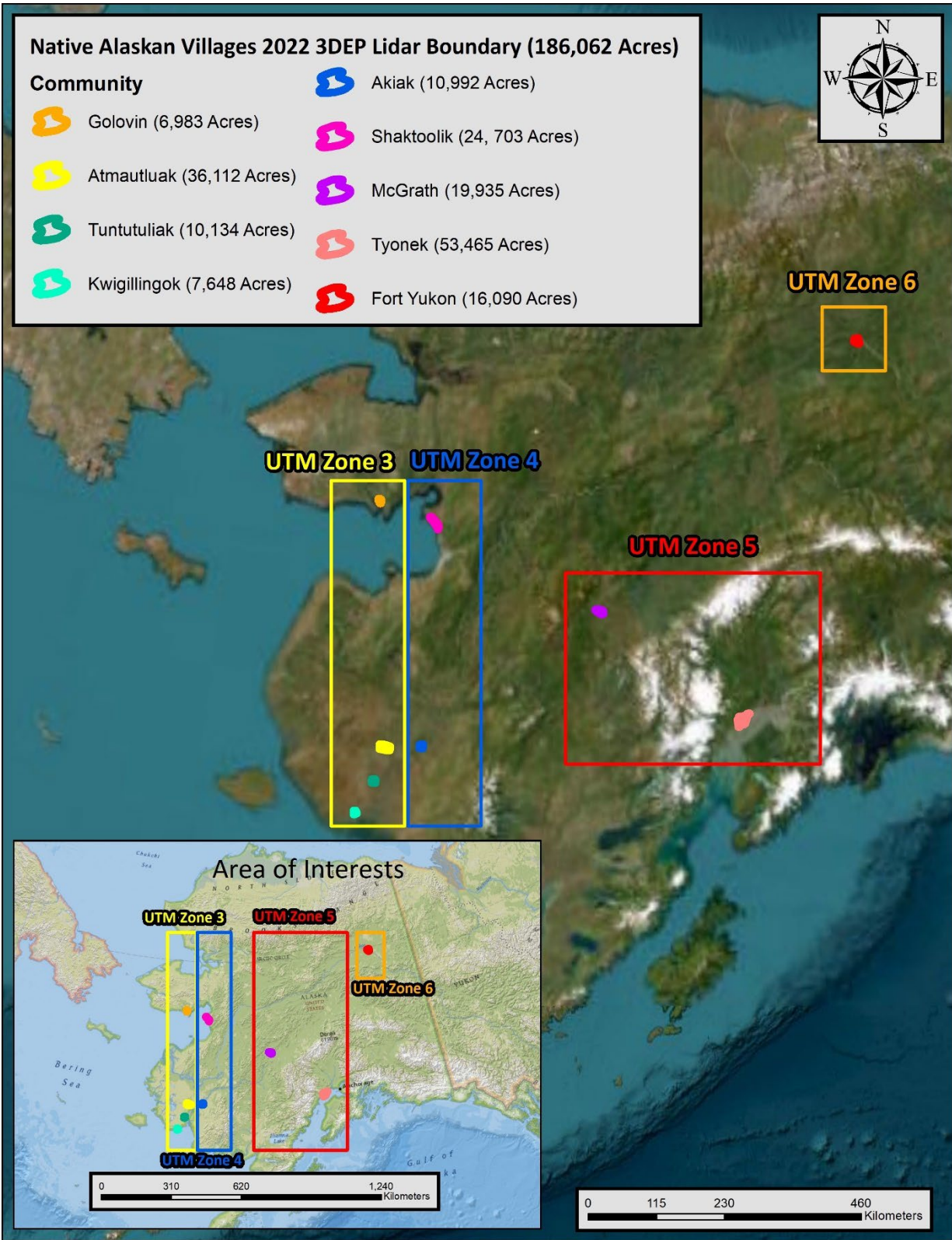


Figure 1: Location map of the Native Villages site in Alaska

ACQUISITION

DOWL’s ground acquisition equipment set up in the Golovin AOI in the Native Villages Lidar study area in Alaska.



Planning

In preparation for data collection, NV5 Geospatial reviewed the project area and developed a specialized flight plan to ensure complete coverage of the Native Villages lidar study area at the target point density of ≥ 2.0 points/m². Acquisition parameters including orientation relative to terrain, flight altitude, pulse rate, scan angle, and ground speed were adapted to optimize flight paths and flight times while meeting all contract specifications. Figure 2 and Figure 3 show these optimized flight paths and dates.

Factors such as satellite constellation availability and weather windows must be considered during the planning stage. The Shaktoolik village was acquired using a Cessna Conquest, while the rest of the lidar data was acquired using a Cessna Caravan. Any weather hazards or conditions affecting the flight were continuously monitored due to their potential impact on the daily success of airborne and ground operations. In addition, logistical considerations including private property access and potential air space restrictions were reviewed. NV5 Geospatial worked closely with USGS to ensure when and where to fly based on the weather conditions and obtaining permission from the Alaskan Natives associated with each native corporation. Because of this, the project was divided into two separate acquisitions, where this report includes 9 of the 14 AOIs. NV5 plans to acquire the 5 remaining AOIs in the summer of 2023.

Table 4: Flight Date Table

Date	Flight Line Number	Start Time (Adjusted GPS)	End Time (Adjusted GPS)
8/10/2022	600 – 604	344208684	344210398
8/11/2022	100 – 105, 200 – 203, 205 -208, 400 - 403	344215522	344282851
8/13/2022	800 - 804	344455947	344457576
10/14/2022	300 – 303, 500 - 504	349822341	349826647
10/21/2022	700 - 707	350416718	350420093

Airborne Lidar Survey

The lidar survey was accomplished using a Riegl VQ-1560ii-S system mounted in a Cessna Caravan or Conquest. Table 5 summarizes the settings used to yield an average pulse density of ≥ 2 pulses/m² over the Native Villages project area. The Riegl VQ-1560ii-S laser system can record unlimited range measurements (returns) per pulse, however a maximum of 15 returns can be stored due to LAS v1.4 file limitations. The typical number of returns digitized from a single pulse range from 1 to 5 for the UTM zone 3, 1 to 7 for the UTM zone 4, and 1 to 8 for UTM Zone 5 and 6 in the Native Villages project area. It is not uncommon for some types of surfaces (e.g., dense vegetation or water) to return fewer pulses to the lidar sensor than the laser originally emitted. The discrepancy between first return and overall delivered density will vary depending on terrain, land cover, and the prevalence of water bodies. All discernible laser returns were processed for the output dataset. Figure 2 and Figure 3 show the flightlines acquired using these lidar specifications.

Table 5: Lidar specifications and survey settings

Parameter	NIR Laser
Acquisition Dates	8/10 – 10/14, 2022
Aircraft Used	Cessna Conquest & Caravan
Sensor	Riegl
Laser	VQ-1560ii-S
Maximum Returns	15
Resolution/Density	Average 2 pulses/m ²
Nominal Pulse Spacing	0.71 m
Survey Altitude (AGL)	2500 m
Survey speed	145 knots
Field of View	58.5°
Mirror Scan Rate	Uniform Point Spacing
Target Pulse Rate	757 kHz
Pulse Length	3 ns
Laser Pulse Footprint Diameter	57.5 cm
Central Wavelength	1064 nm
Pulse Mode	Multiple Times Around (MTA)
Beam Divergence	0.23 mrad
Swath Width	2800 m
Swath Overlap	20%
Intensity	16-bit
Vertical Accuracy	RMSE _z (Non-Vegetated) ≤ 10 cm
NVA Accuracy	NVA (95% Confidence Level) ≤ 19.6 cm
VVA Accuracy	VVA (95 th Percentile) ≤ 30 cm



Riegl VQ-1560ii-S

All areas were surveyed with an opposing flight line side-lap of $\geq 20\%$. To accurately solve for laser point position (geographic coordinates x, y and z), the positional coordinates of the airborne sensor and the orientation of the aircraft to the horizon (attitude) were recorded continuously throughout the lidar data collection mission. Position of the aircraft was measured twice per second (2 Hz) by an onboard differential GPS unit, and aircraft attitude was measured 200 times per second (200 Hz) as pitch, roll and yaw (heading) from an onboard inertial measurement unit (IMU). To allow for post-processing correction and calibration, aircraft and sensor position and attitude data are indexed by GPS time.

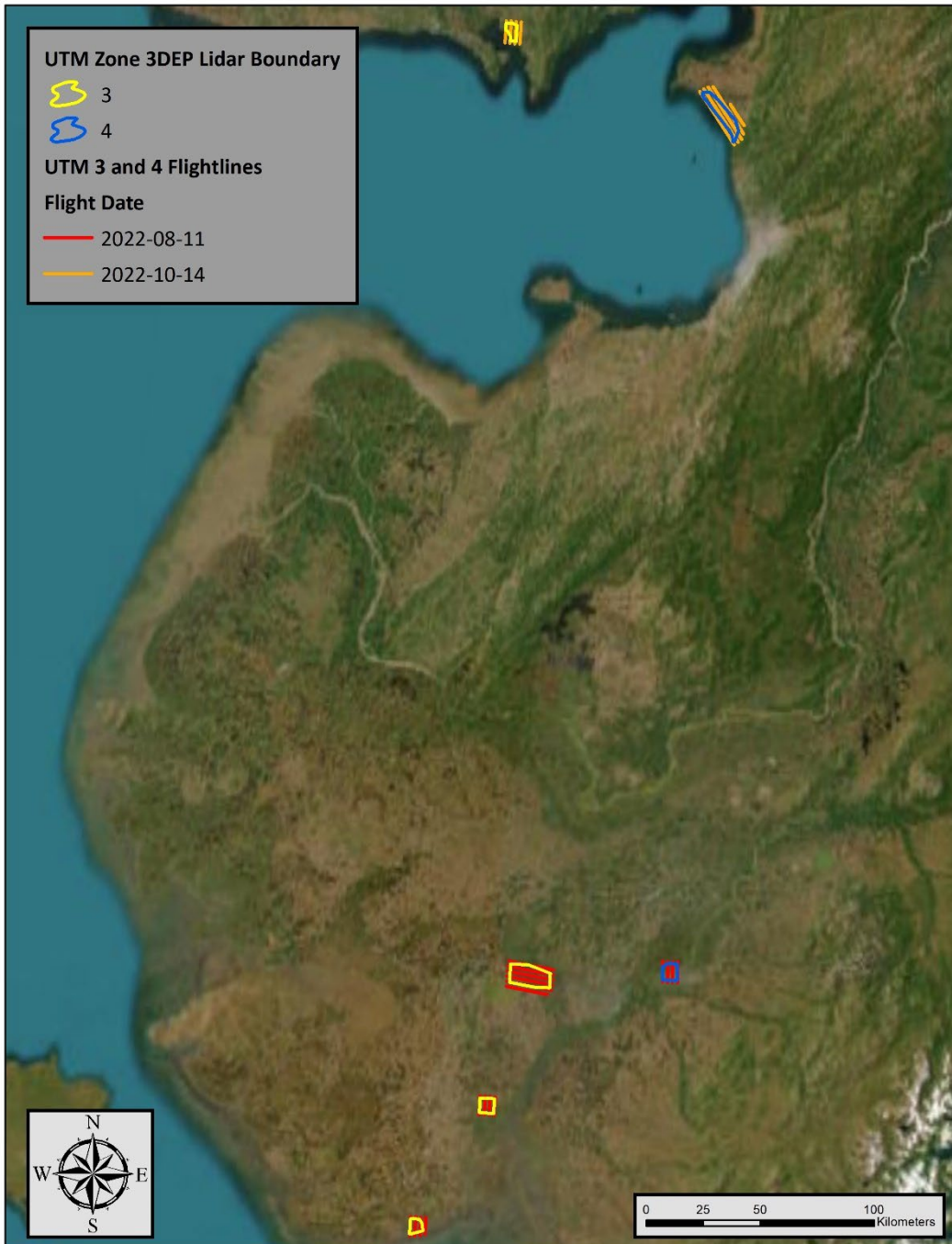


Figure 2: Flightlines map for projection zones 3 and 4

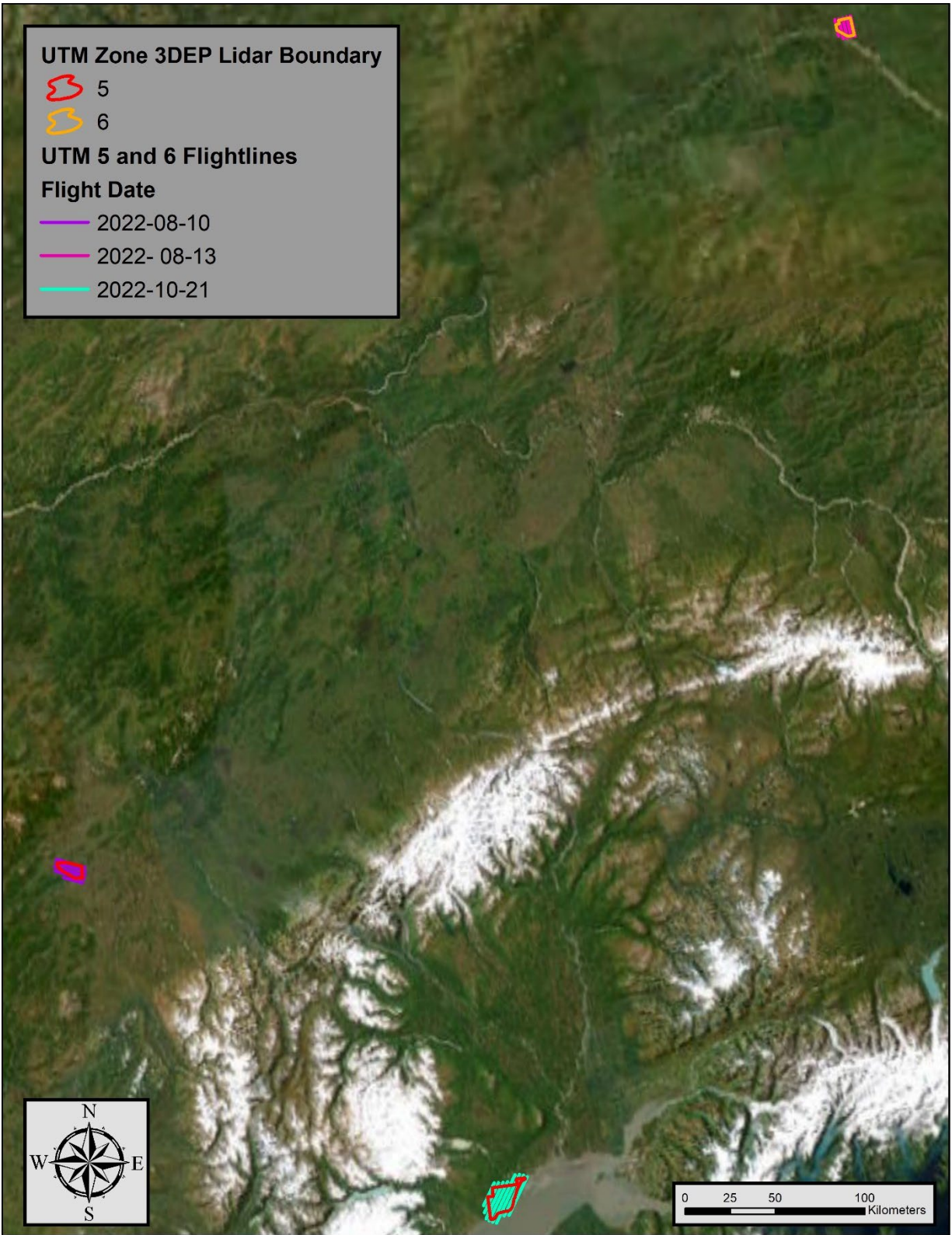


Figure 3: Flightlines map for projection zones 5 and 6

Ground Survey

Ground control surveys, including monumentation, and ground survey points (GSPs) were conducted by DOWL to support the airborne acquisition. DOWL’s ground survey report’s for each AOI (Akiak, Atmaultluak, Fort Yukon, Golovin, Kwigillingok, McGrath, Shaktoolik, Tuntutuliak, and Tyonek) are included with this delivery as “1127.63642.01 USGS Mapping” followed by the name of the AOI – e.g. “1127.63642.01 USGS Mapping Akiak”. The locations of the survey points are shown in Figure 4.



Existing NGS Monument



DOWL-Established Monument

Base Stations

Base stations were used for collection of ground survey points using post processed kinematic (PPK) survey techniques.

Base station locations were selected by DOWL with consideration for satellite visibility, field crew safety, and optimal location for GSP coverage. These base stations were given to NV5 for processing, and accuracy calculations which are shown below in Table 6. DOWL established and used previously established monuments including some National Geodetic Survey (NGS) monuments.

Table 6: Base station positions for the Native Villages acquisition. Coordinates are on the NAD83 (2011) datum, epoch 2010.00

Monument ID	Latitude	Longitude	Ellipsoid (meters)
ATT-1	60° 51' 55.27908"	-162° 16' 30.47383"	14.360
4A2 C (SACS)	60° 51' 48.59171"	-162° 16' 28.71678"	13.884
GLV-1	64° 32' 56.50987"	-163° 00' 47.62518"	24.016
USLM 3651	64° 32' 41.11088"	-163° 01' 49.41365"	33.374
KWK-1	59° 52' 34.19692"	-163° 10' 02.61470"	15.493
946 5911A (BBGM54)	59° 52' 45.53920"	-163° 08' 56.26612"	15.673
GGV A (BBFB70)	59° 52' 33.64326"	-163° 09' 59.51655"	14.704
WTL-1	60° 21' 03.56198"	-162° 39' 25.18482"	17.462
946 6197 B	60° 20' 33.62284"	-162° 40' 58.58820"	15.422
AKI-1	60° 54' 21.63673"	-161° 13' 34.92000"	20.426
OPUS DB BBHL91	60° 54' 18.25980"	-161° 13' 40.09464"	20.643
SKK-1	64° 22' 03.94118"	-161° 13' 23.43132"	13.829
946 8691 D	64° 22' 40.51694"	-161° 14' 08.44455"	11.654
MCG-1	62° 57' 28.25651"	-155° 35' 53.70823"	114.297
MCG-2	62° 55' 14.14434"	-155° 26' 56.26932"	153.650
MCG A	62° 57' 27.74232"	-155° 36' 12.71573"	113.524
McGrath W. Base	62° 57' 18.20952"	-155° 36' 09.27536"	113.994
TYE-1	61° 07' 28.24450"	-151° 05' 37.44324"	34.398
Terrace	61° 09' 29.72565"	-151° 03' 05.89523"	29.202
FYU B	66° 34' 05.09664"	-145° 15' 40.62983"	140.501

Ground Survey Points (GSPs)



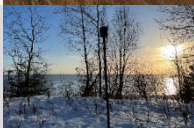



Ground survey points were collected using post-processed kinematic (PPK) survey techniques. PPK surveys compute these corrections during post-processing to achieve comparable accuracy. PPK surveys record data while stationary for at least five seconds, calculating the position using at least three one-second epochs

GSPs were collected in areas where good satellite visibility was achieved on paved roads and other hard surfaces such as gravel or packed dirt roads. GSP measurements were not taken on highly reflective surfaces such as center line stripes or lane markings on roads due to the increased noise seen in the laser returns over these surfaces. GSPs were collected within as many flightlines as possible; however, the distribution of GSPs depended on ground access constraints and monument locations and may not be equably distributed throughout the study area (Figure 4).

Land Cover Class

In addition to ground survey points, DOWL collected land cover class check points throughout the study area to evaluate vertical accuracy. NV5 Geospatial calculated the vertical accuracy statistics for all land cover types to assess confidence in the lidar derived ground models across land cover classes (Table 7, see Lidar Accuracy Assessments, page 34).

Table 7: Land Cover Types and Descriptions

Land cover type	Land cover code	Example	Description	Accuracy Assessment Type
Shrub	SH		Low growth shrub	VVA
Tall Grass	TG		Herbaceous grasslands in advanced stages of growth	VVA
Forest	FR		Forested areas	VVA
Bare Earth	BE		Areas of bare earth surface	NVA
Urban	UA		Areas dominated by urban development, including parks	NVA
Tundra	TU		Flat, treeless area where the soil is permanently frozen	NVA

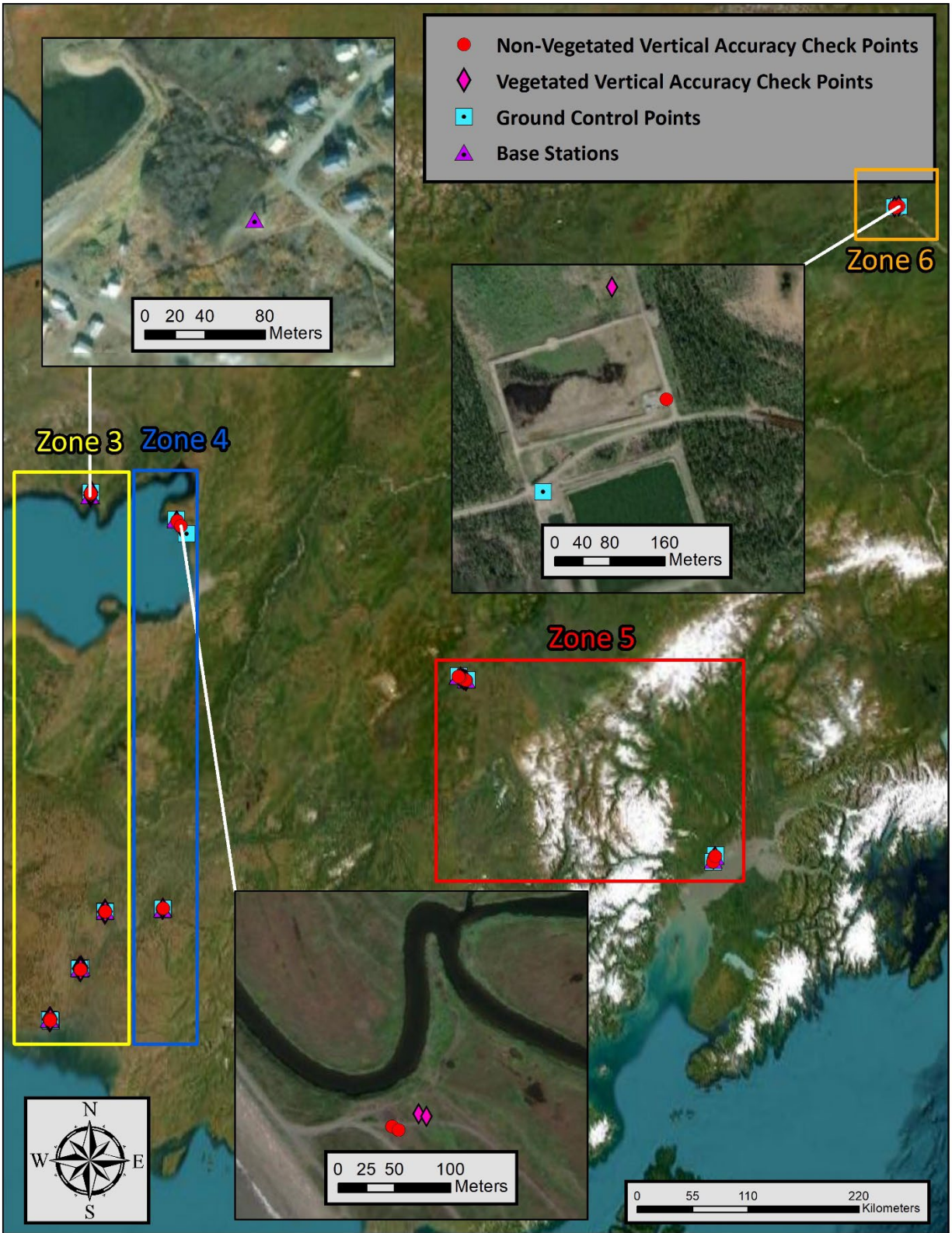


Figure 4: Ground survey location map

This 50 meter lidar cross section shows a view of a bridge, water, and buildings in the Kwigillingok village for the Native Villages landscape, colored by point classification.

- Ground
- Default
- Bridge
- Water
- Buildings/Anthropogenic Features



NIR Lidar Data

Applanix + POSPac software was used for post-processing of airborne GPS and inertial data (IMU), which is critical to the positioning and orientation of the lidar sensor during all flights. Applanix POSPac combines aircraft raw trajectory data with stationary GPS base station data yielding a “Smoothed Best Estimate Trajectory” (SBET) necessary for additional post processing software to develop the resulting geo-referenced point cloud from the lidar missions (Table 9). SBET quality reports for each processing group have been provided in the file “SBET_QC_Reports.zip” that accompanies this report.

During the sensor trajectory processing (combining GPS & IMU datasets) certain statistical graphs and tables are generated within the Applanix POSPac processing environment which are commonly used as indicators of processing stability and accuracy. This data for analysis includes max horizontal and vertical GPS variance, separation plot, altitude plot, PDOP plot, base station baseline length, processing mode, number of satellite vehicles, and mission trajectory.

Point clouds were created using the RiPROCESS software. The generated point cloud is the mathematical three dimensional composite of all returns from all laser pulses as determined from the aerial mission. The point cloud is imported into GeoCue distributive processing software. Imported data is tiled and then calibrated using TerraMatch and proprietary software. Using TerraScan, the vertical accuracy of the surveyed ground control is tested and any bias is removed from the data. TerraScan and TerraModeler software packages are then used for automated data classification and manual cleanup. The data are manually reviewed and any remaining artifacts removed using functionality provided by TerraScan and TerraModeler.

DEMs and Intensity Images are then generated using NV5 Geospatial proprietary software. In the bare earth surface model, above-ground features are excluded from the data set. ESRI ArcMap and Global Mapper are used as a final check of the bare earth dataset. Finally, proprietary software is used to perform statistical analysis of the LAS files (Table 8).

Table 8: Software used for statistical analysis

Statistical Software	Version
Applanix + POSPac	8.7
LASMonkey	2.6.7
RiPROCESS	1.8.6
GeoCue	2020.1.22.1
ESRI Arc Map	10.8
TerraModeler	21.008
TerraScan	21.016

Table 9: Lidar processing workflow

Lidar Processing Step	Software Used
Resolve kinematic corrections for aircraft position data using kinematic aircraft GPS and static ground GPS data. Develop a smoothed best estimate of trajectory (SBET) file that blends post-processed aircraft position with sensor head position and attitude recorded throughout the survey.	POSPac MMS v.8.7
Calculate laser point position by associating SBET position to each laser point return time, scan angle, intensity, etc. Create raw laser point cloud data for the entire survey in *.las (ASPRS v. 1.4) format. Convert data to orthometric elevations by applying a geoid correction.	RiUnite v.1.0.3
Import raw laser points into manageable blocks to perform manual relative accuracy calibration and filter erroneous points. Classify ground points for individual flight lines.	TerraScan v.19.005
Using ground classified points per each flight line, test the relative accuracy. Perform automated line-to-line calibrations for system attitude parameters (pitch, roll, heading), mirror flex (scale) and GPS/IMU drift. Calculate calibrations on ground classified points from paired flight lines and apply results to all points in a flight line. Use every flight line for relative accuracy calibration.	StripAlign v.2.21
Classify resulting data to ground and other client designated ASPRS classifications (Table 10). Assess statistical absolute accuracy via direct comparisons of ground classified points to ground control survey data.	TerraScan v.19.005 TerraMatch v. 19.002 TerraModeler v.19.003
Generate bare earth models as triangulated surfaces. Generate highest hit models as a surface expression of all classified points. Export all surface models as Cloud Optimized GeoTIFFs at a 1 meter pixel resolution.	LAS Product Creator 3.0 (NV5 Geospatial proprietary) ArcMap v. 10.8

Table 10: ASPRS LAS classification standards applied to the Native Villages dataset

Classification Number	Classification Name	UTM Zone 3 Point Count	UTM Zone 4 Point Count	UTM Zone 5 Point Count	UTM Zone 6 Point Count	Classification Description
1	Default/Unclassified	358,962,926	354,281,366	1,225,370,635	411,041,974	Laser returns that are not included in the ground class, composed of vegetation and anthropogenic features
1-W	Edge Clip/Withheld	72,170,398	45,883,684	106,688,822	33,757,589	Laser returns at the outer edges of flightlines that are geometrically unreliable
2	Ground	790,961,501	460,178,821	985,665,565	193,052,029	Laser returns that are determined to be ground using automated and manual cleaning algorithms
6	Buildings	906,326	256,060	787,975	484,038	Permanent structures such as buildings determined using automated cleaning algorithms
7-W	Low Noise/Withheld	756,563	479,249	1,695,788	243,326	Laser returns that are often associated with artificial points below the ground surface
9	Water	44,752,993	43,019,223	7,793,050	8,049,701	Laser returns that are determined to be water using automated and manual cleaning algorithms
11	Road Surface	459,337	190,328	4,406,540	1,399,619	Surfaces determined to be traveled by four-wheeled traffic were digitized and classed as roads, excluding runways and cleared vegetation areas.
17	Bridge	147,500	301	2,624	2,098	Bridge decks
18-W	High Noise	1,687,209	579,427	3,107,368	218,888	Laser returns that are often associated with birds, scattering from reflective surfaces.
20	Ignored Ground	4,098,053	1,594,003	1,049,859	494,631	Ground points proximate to water's edge breaklines; ignored for correct model creation

Feature Extraction

Hydroflattening and Water's Edge Breaklines

The ocean surrounding the Native Villages and other water bodies within the project area were flattened to a consistent water level. Bodies of water that were flattened include lakes and other closed water bodies with a surface area greater than 2 acres, all streams and rivers that are nominally wider than 30 meters, all tidal and non-tidal waters bordering the project, and select smaller bodies of water as feasible. The hydroflattening process eliminates artifacts in the digital terrain model caused by both increased variability in ranges or dropouts in laser returns due to the low reflectivity of water.

Hydroflattening of closed water bodies was performed through a combination of automated and manual detection and adjustment techniques designed to identify water boundaries and water levels. Boundary polygons were developed using an algorithm which weights lidar-derived slopes, intensities, and return densities to detect the water's edge. The water edges were then manually reviewed and edited as necessary. Specific care was taken to not hydroflatten wetland and marsh habitat found throughout the study site.

Once polygons were developed the initial ground classified points falling within water polygons were reclassified as water points to omit them from the final ground model. Elevations were then obtained from the filtered lidar returns to create the final breaklines. Lakes were assigned a consistent elevation for an entire polygon while rivers were assigned consistent elevations on opposing banks and smoothed to ensure downstream flow through the entire river channel.

Water boundary breaklines were then incorporated into the hydroflattened DEM by enforcing triangle edges (adjacent to the breakline) to the elevation values of the breakline. This implementation corrected interpolation along the hard edge. Water surfaces were obtained from a TIN of the 3-D water edge breaklines resulting in the final hydroflattened model (Figure 5).

Hydro-Flattened Raster DEM Processing

Hydro-Flattened DEMs (topographic) represent a lidar-derived product illustrating the grounded terrain and associated breaklines (as described above) in raster format. NV5 Geospatial's proprietary software was used to take all input sources (bare earth lidar points, bridge and hydro breaklines, etc.) and create a Triangulated Irregular Network (TIN) on a tile-by-tile basis. Data extending past the tile edge is incorporated in this process so that triangulation can occur without creating edge artifacts. From the TIN, linear interpolation is used to calculate the cell values for the raster product. The raster product is then clipped along the tile edge to remove areas that overlap with adjacent tiles. A 32-bit floating point GeoTIFF DEM was generated for each tile with a pixel size of 1.0-meter. NV5 Geospatial's proprietary software was used to write appropriate horizontal and vertical coordinate reference system (CRS) information as well as applicable header values into the file during product generation. Each DEM is reviewed in Global Mapper and ESRI ArcMap to check for any surface anomalies and to ensure a seamless dataset. NV5 Geospatial ensures there are no void or no-data values (-999999) in each derived DEM. This is achieved by using propriety software checking all cell values that fall within the project boundary. NV5 Geospatial uses a proprietary tool called FOCUS on Delivery to check all formatting requirements of the DEMs against what is required before final delivery.

Dams

The study area contains numerous dams, which made the hydroflattening process unusually complex. Hydroflattening was treated on a case-by-case basis as to how to best represent the change in elevation within hydroflattened features. The damming features, as in the case of beaver dams or other natural causes, were not tall or wide enough to be adequately captured as being distinct from the ground model. This is specifically because the ground proximate to breaklines was ignored (assigned class 20) for proper implementation. In select locations, this led to some flattened waterbodies appearing unconstrained. Upon review of these situations, only the waterbody features in the ground model deemed to be an appropriate representation of the actual feature were left unconstrained when trying to anticipate future modeling applications.

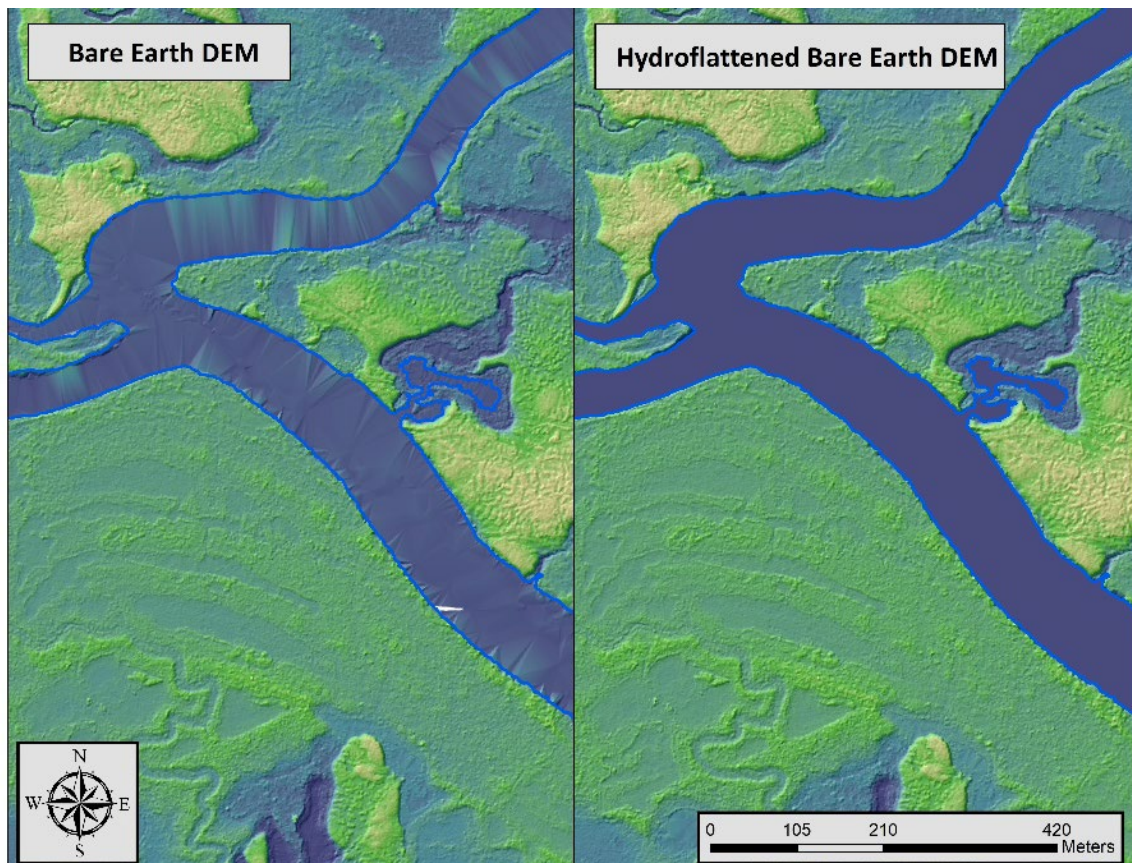


Figure 5: Example of hydroflattening in the Native Villages Lidar dataset

Roads

Ground surface models generated from the lidar data collection were used for cross-validation in areas of unobstructed canopy. Single line vectors were digitized for each road feature regardless of lanes of travel. Due to the large number of unimproved dirt roads serving agricultural and rural areas, connectivity of these roads was not interpolated in areas undeterminable through lidar data or imagery. Gravel and dirt that were determined to be traveled by four-wheeled traffic indicated by tracks were digitized and classed as roads, excluding runways and cleared vegetation areas (Figure 6a).

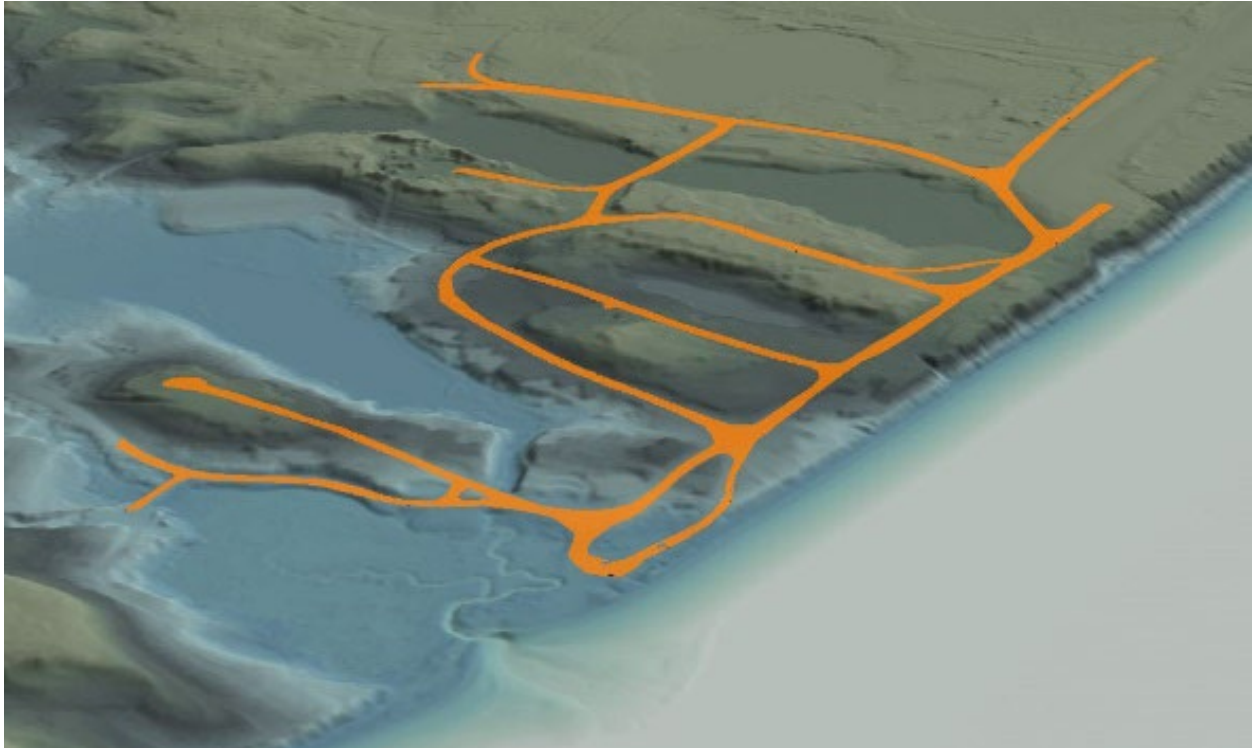


Figure 6: Sample Image of road surface lidar classified points (orange lines) within the Native Villages boundary.

Intensity Image Processing

Intensity images represent reflectivity values collected by the lidar sensor during acquisition. NV5 Geospatial proprietary software generates intensity images using all valid first returns and excluding those flagged with a withheld bit. Intensity images are linearly scaled to a value range specific to the project area and sensor to standardize the images and reduce differences between individual flightlines. Appropriate horizontal projection information as well as applicable header values are written during product generation. NV5 Geospatial uses a proprietary tool called FOCUS on Delivery to check all formatting requirements of the images against what is required before final delivery.

Swath Separation Raster Processing

Swath Separation Images are rasters that represent the interswath alignment between flight lines and provide a qualitative evaluation of the positional quality of the point cloud. NV5 Geospatial proprietary software generated 1-meter raster images in GeoTIFF format using the first returns from all the classes (Table 10), excluding points flagged with the withheld bit, and using a grid based average algorithm. Images are generated with 75% intensity opacity and four absolute 8-cm intervals (see Figure 7 below for interval coloring). Intensity images are linearly scaled to a value range specific to the project area and sensor to standardize the images and reduce differences between individual flightlines. Appropriate horizontal projection information as well as applicable header values are written to the file during product generation. NV5 Geospatial uses a proprietary tool called FOCUS on Delivery to check all formatting requirements of the images against what is required before final delivery.

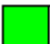



	0-8cm
	8-16cm
	16-24cm
	>24cm

Figure 7: The color ramp values used in the Native Villages project

Maximum Surface Height Raster Processing

Maximum Surface Height rasters (topographic) represent a lidar-derived product illustrating natural and built-up features. NV5 Geospatial's proprietary software was used to take all valid classified lidar points, excluding those flagged with a withheld bit, and create a raster on a tile-by-tile basis. Data extending past the tile edge is incorporated in this process so that proper gridding can occur. The raster product is then clipped back to the tile edge so that no overlapping cells remain across the project area. A 32-bit floating point GeoTIFF was generated for each tile with a pixel size of 1-meter. NV5 Geospatial's proprietary software was used to write appropriate horizontal and vertical projection information as well as applicable header values into the file during product generation. Each maximum surface height raster is reviewed in ESRI ArcMap to check for any anomalies and to ensure a seamless dataset. NV5 Geospatial uses a proprietary tool called FOCUS on Delivery to check all formatting requirements of the DEMs against what is required before final delivery.

RESULTS & DISCUSSION

This 35 meter lidar cross section shows a view of two bridges in Kwigillingok for the Native Villages project, colored by point laser echo.

- Only Echo
- First of Many
- Intermediate
- Last of Many



Lidar Density

The acquisition parameters were designed to acquire an average first-return density of 2 points/m². First return density describes the density of pulses emitted from the laser that return at least one echo to the system. Multiple returns from a single pulse were not considered in first return density analysis. Some types of surfaces (e.g., breaks in terrain, water and steep slopes) may have returned fewer pulses than originally emitted by the laser. First returns typically reflect off the highest feature on the landscape within the footprint of the pulse. In forested or urban areas, the highest feature could be a tree, building or power line, while in areas of unobstructed ground, the first return will be the only echo and represents the bare earth surface.

The density of ground-classified lidar returns was also analyzed for this project. Terrain character, land cover, and ground surface reflectivity all influenced the density of ground surface returns. In vegetated areas, fewer pulses may penetrate the canopy, resulting in lower ground density.

Table 11 depicts the average first return and ground classified densities by UTM zone. The UTM 3 zone data yielded the lowest average first point density return (4.78 points/m²), while the UTM 6 zone data yielded the highest average first point density return (5.93 points/m²). The lowest and highest average ground classified return point densities were, respectively, 3.01 for UTM zone 6 and 3.44 for UTM zone 4. The statistical distributions are represented in Figure 8 through Figure 15, while the spatial distributions of first return point densities and ground classified return densities per 100 m x 100 m cell are portrayed in Figure 16 and Figure 17.

Table 11: Average lidar point densities

UTM Zone	Classification	Point Density
3	First-Return	4.78 points/m ²
	Ground Classified	3.41 points/m ²
4	First-Return	5.20 points/m ²
	Ground Classified	3.44 points/m ²
5	First-Return	5.78 points/m ²
	Ground Classified	3.35 points/m ²
6	First-Return	5.93 points/m ²
	Ground Classified	3.01 points/m ²

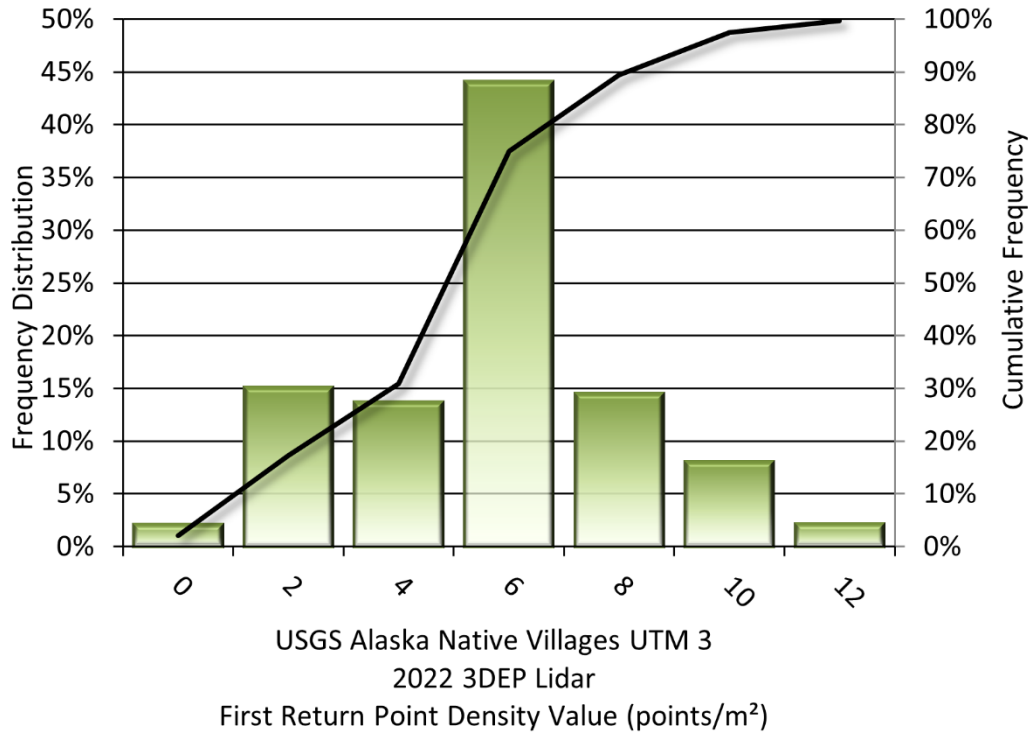


Figure 8: Frequency distribution of first return point density values per 100 x 100 m cell for UTM 3

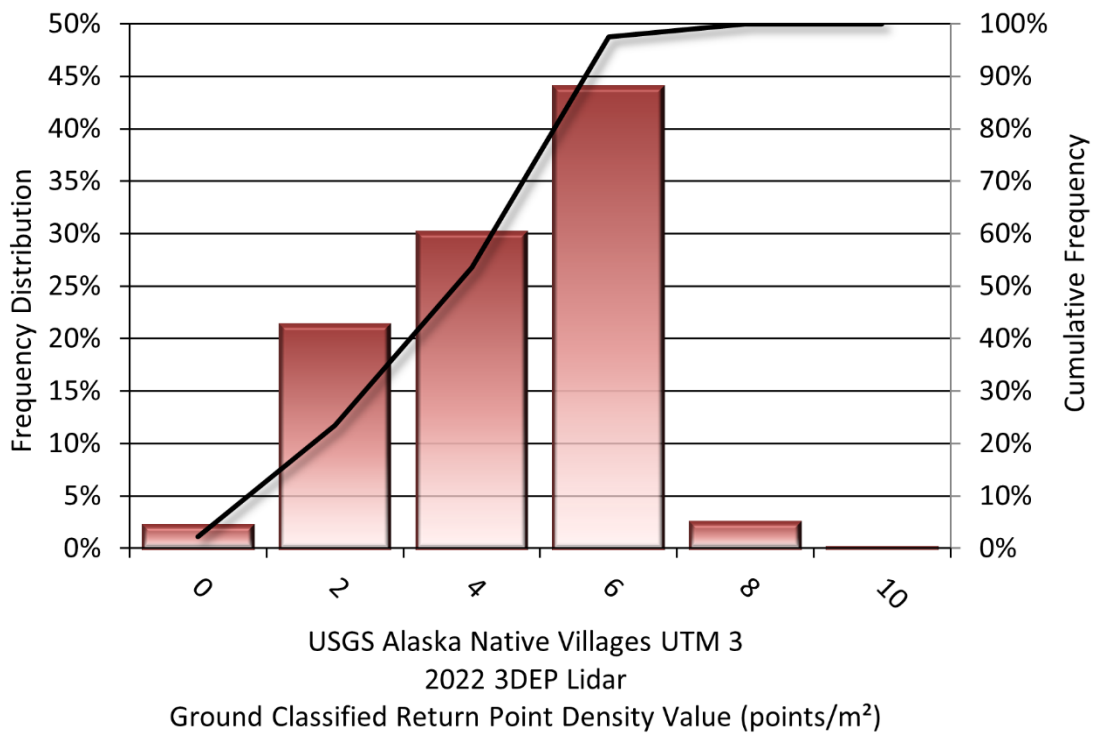


Figure 9: Frequency distribution of ground-classified return point density values per 100 x 100 m cell for UTM 3

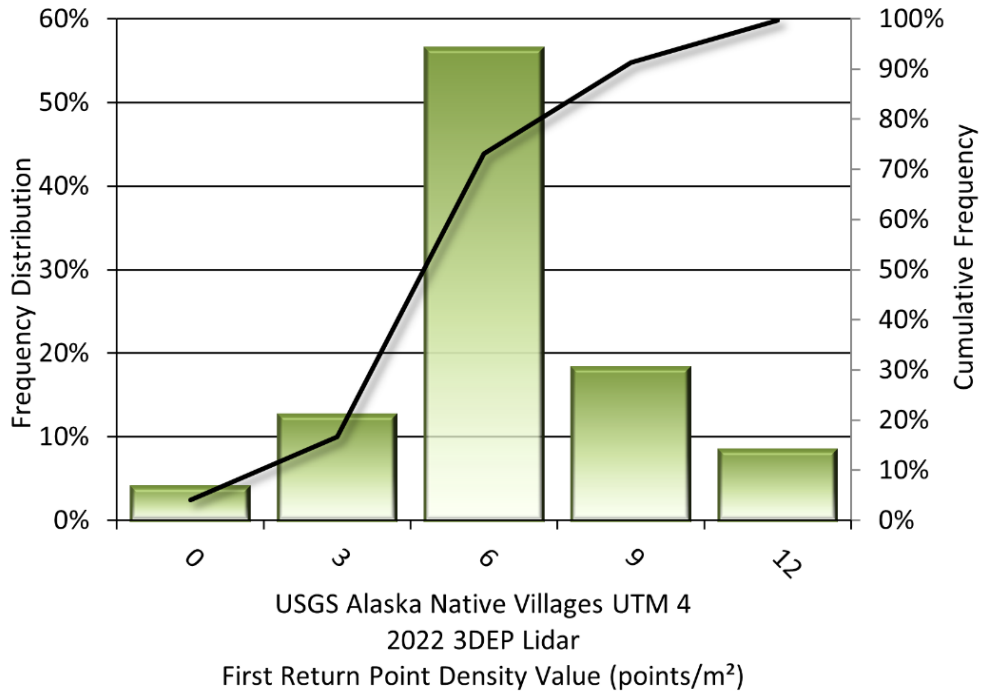


Figure 10: Frequency distribution of ground-classified return point density values per 100 x 100 m cell for UTM 4

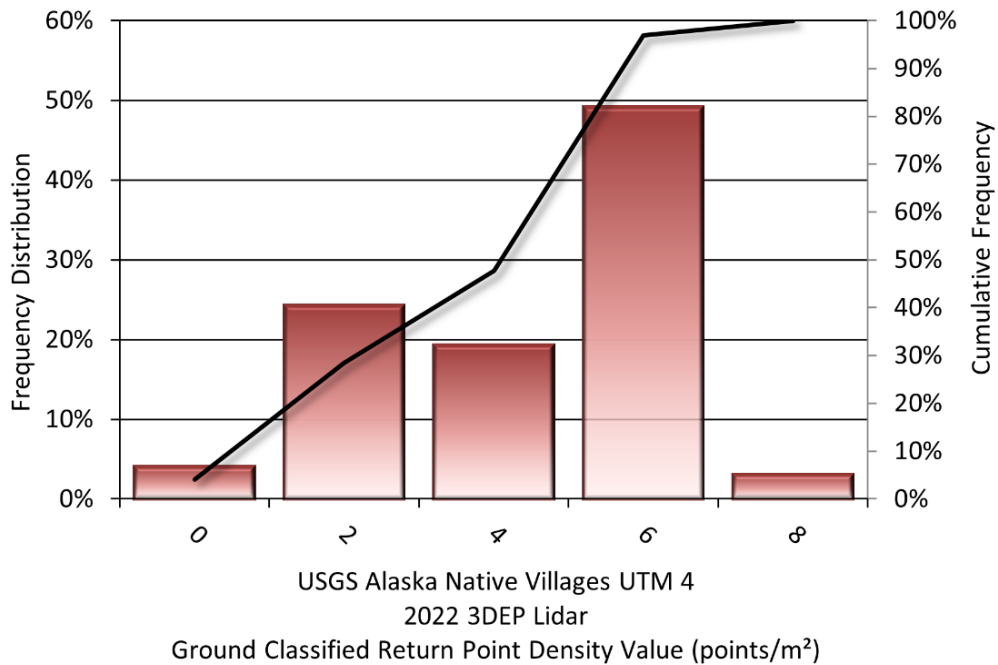


Figure 11: Frequency distribution of ground-classified return point density values per 100 x 100 m cell for UTM 4

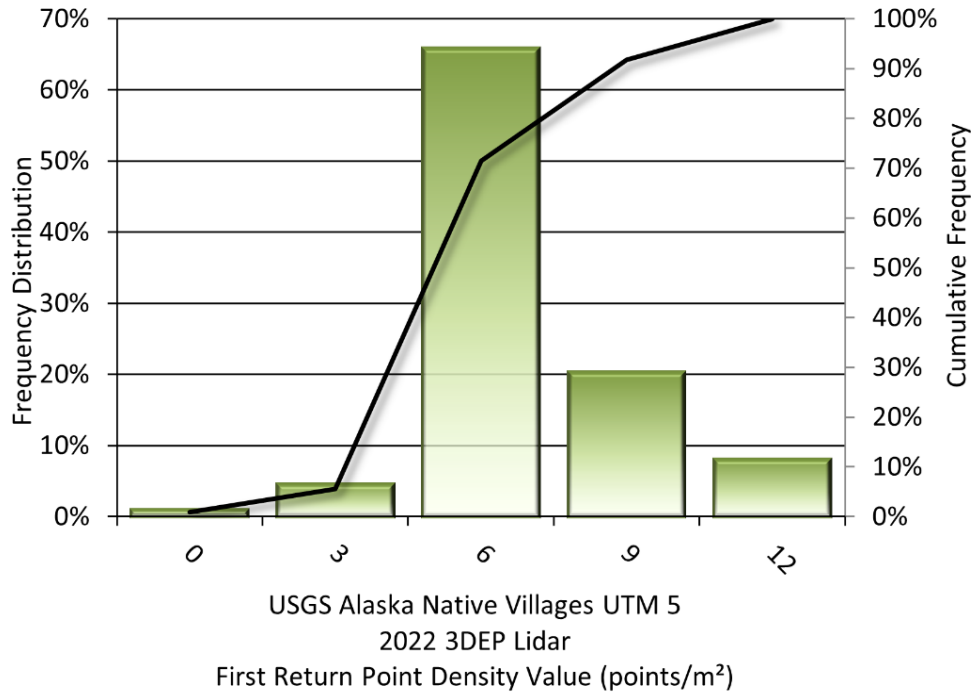


Figure 12: Frequency distribution of ground-classified return point density values per 100 x 100 m cell for UTM 5

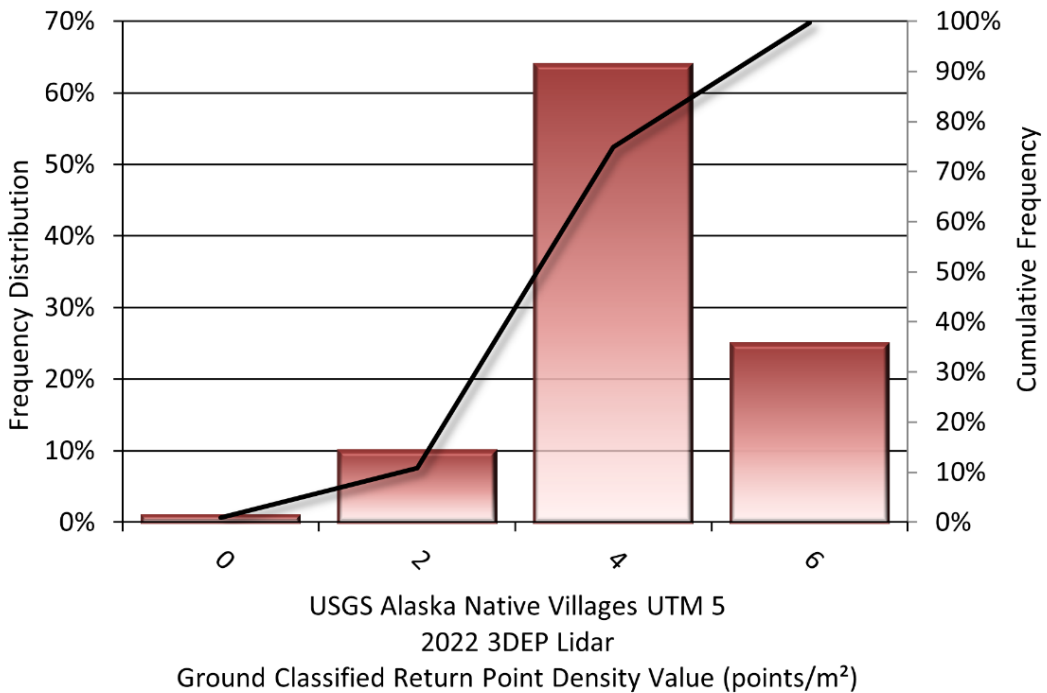


Figure 13: Frequency distribution of ground-classified return point density values per 100 x 100 m cell for UTM 5

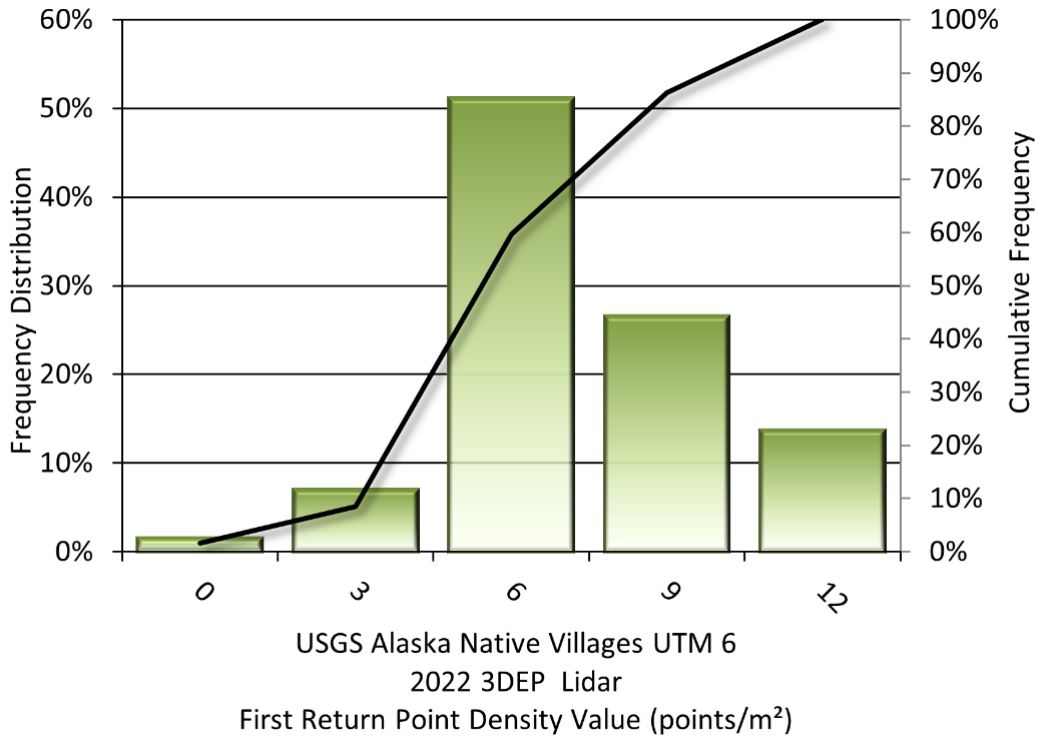


Figure 14: Frequency distribution of ground-classified return point density values per 100 x 100 m cell for UTM 6

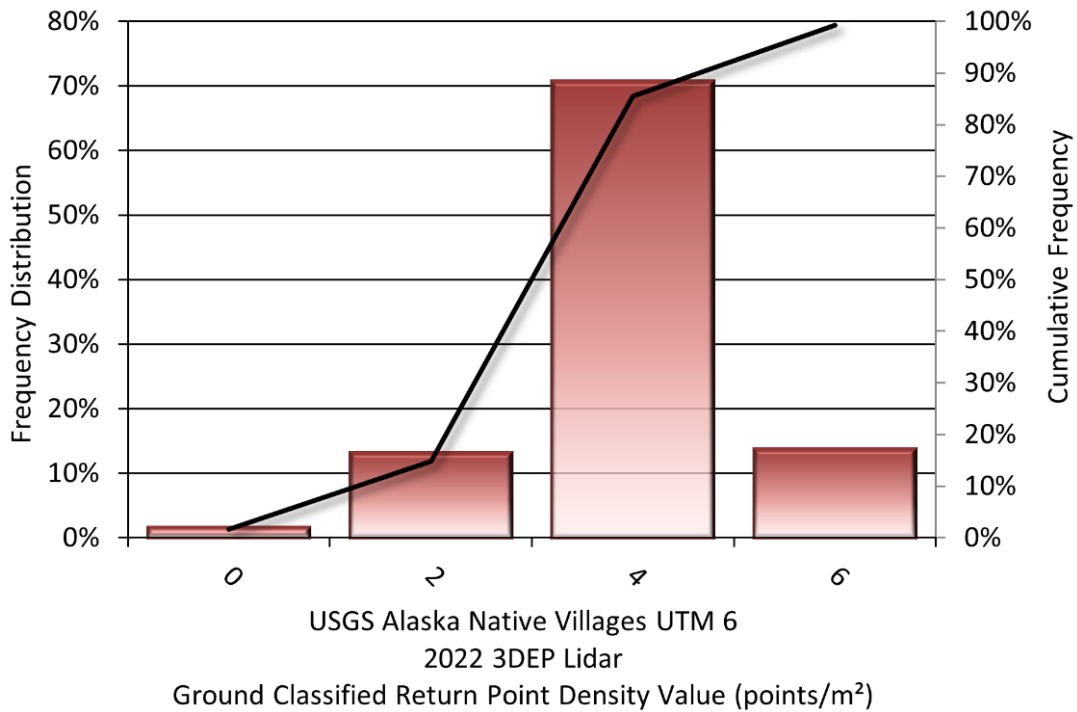


Figure 15: Frequency distribution of ground-classified return point density values per 100 x 100 m cell for UTM 6

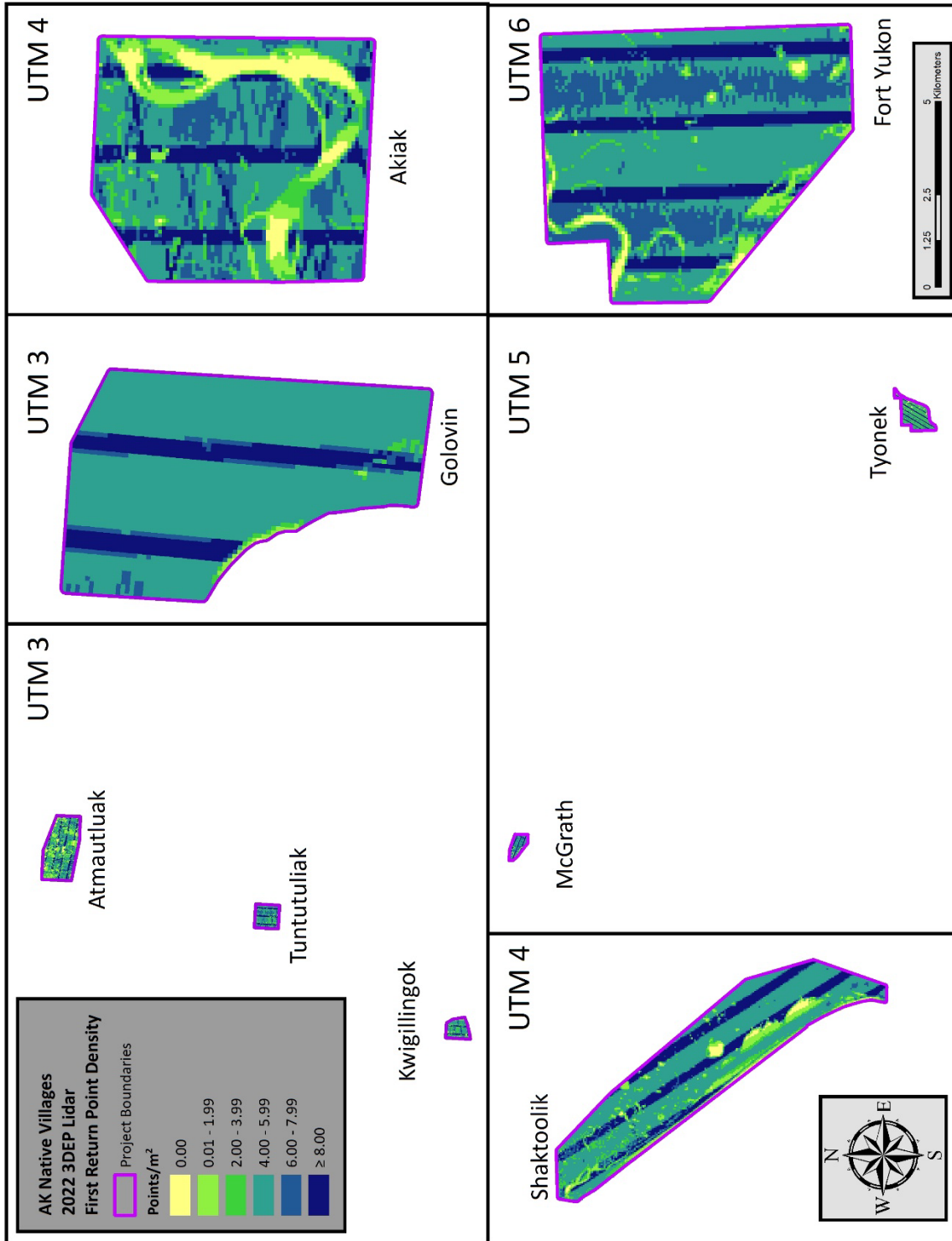


Figure 16: First return point density map for the Native Villages sites (100 m x 100 m cells)

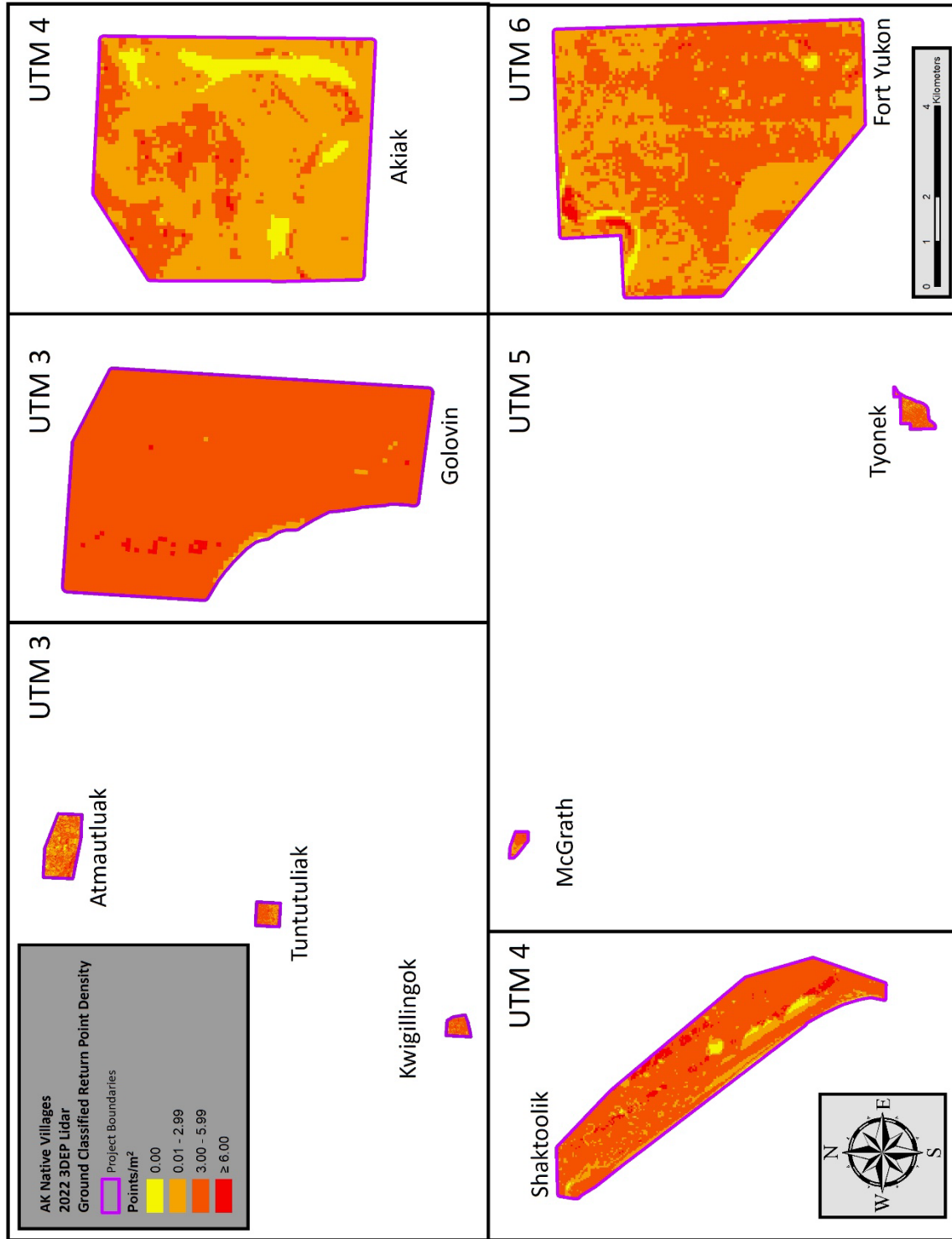


Figure 17: Ground classified point density map for the Native Villages sites (100 m x 100 m cells)

Lidar Accuracy Assessments

The accuracy of the lidar data collection can be described in terms of absolute accuracy (the consistency of the data with external data sources) and relative accuracy (the consistency of the dataset with itself). See Appendix A for further information on sources of error and operational measures used to improve relative accuracy.

Lidar Non-Vegetated Vertical Accuracy

Absolute accuracy was assessed using Non-Vegetated Vertical Accuracy (NVA) reporting designed to meet guidelines presented in the FGDC National Standard for Spatial Data Accuracy¹. NVA compares known ground check point data that were withheld from the calibration and post-processing of the lidar point cloud to the triangulated surface generated by the classified lidar point cloud (Figure 18, Figure 21, Figure 24, Figure 27) as well as the derived gridded bare earth DEM (Figure 19, Figure 22, Figure 25, and Figure 28). NVA is a measure of the accuracy of lidar point data in open areas where the lidar system has a high probability of measuring the ground surface and is evaluated at the 95% confidence interval ($1.96 * RMSE$), as shown in Table 12.

The mean and standard deviation (σ) of divergence of the ground surface model from quality assurance point coordinates are also considered during accuracy assessment. These statistics assume the error for x, y and z is normally distributed, and therefore the skew and kurtosis of distributions are also considered when evaluating error statistics. For the Native Villages survey, a total of 45 ground check points were withheld from the calibration and post processing of the lidar point cloud.

NV5 Geospatial also assessed absolute accuracy using 37 ground control points. Although these points were used in the calibration and post-processing of the lidar point cloud, they still provide a good indication of the overall accuracy of the lidar dataset, and therefore have been provided in Table 12 and Figure 20, Figure 23, Figure 26, and Figure 29.

¹ Federal Geographic Data Committee, ASPRS POSITIONAL ACCURACY STANDARDS FOR DIGITAL GEOSPATIAL DATA EDITION 1, Version 1.0, NOVEMBER 2014.
https://www.asprs.org/a/society/committees/standards/Positional_Accuracy_Standards.pdf.

Table 12: Absolute accuracy results

UTM Zone	Parameter	NVA, as compared to classified LAS	NVA, as compared to bare earth DEM	Ground Control Points
3	Sample	17 points	17 points	16 points
	95% Confidence (1.96*RMSE)	0.093 m	0.093 m	0.050 m
	Average	-0.006 m	-0.006 m	0.001 m
	Median	0.001 m	0.001 m	0.002 m
	RMSE	0.047 m	0.047 m	0.025 m
	Standard Deviation (1σ)	0.048 m	0.048 m	0.026 m
4	Sample	10 points	10 points	9 points
	95% Confidence (1.96*RMSE)	0.034 m	0.048 m	0.060 m
	Average	0.007 m	-0.009 m	0.004 m
	Median	0.004 m	-0.009 m	0.004 m
	RMSE	0.017 m	0.024 m	0.031 m
	Standard Deviation (1σ)	0.017 m	0.024 m	0.032 m
5	Sample	15 points	15 points	10 points
	95% Confidence (1.96*RMSE)	0.058 m	0.051 m	0.057 m
	Average	0.009 m	-0.007 m	0.002 m
	Median	0.013 m	0.001 m	0.002 m
	RMSE	0.030 m	0.026 m	0.029 m
	Standard Deviation (1σ)	0.029 m	0.026 m	0.031 m
6	Sample	3 points	3 points	2 points
	95% Confidence (1.96*RMSE)	0.026 m	0.026 m	0.024 m
	Average	0.000 m	-0.006 m	0.005 m
	Median	-0.004 m	-0.006 m	0.005 m
	RMSE	0.013 m	0.013 m	0.012 m
	Standard Deviation (1σ)	0.016 m	0.015 m	0.016 m

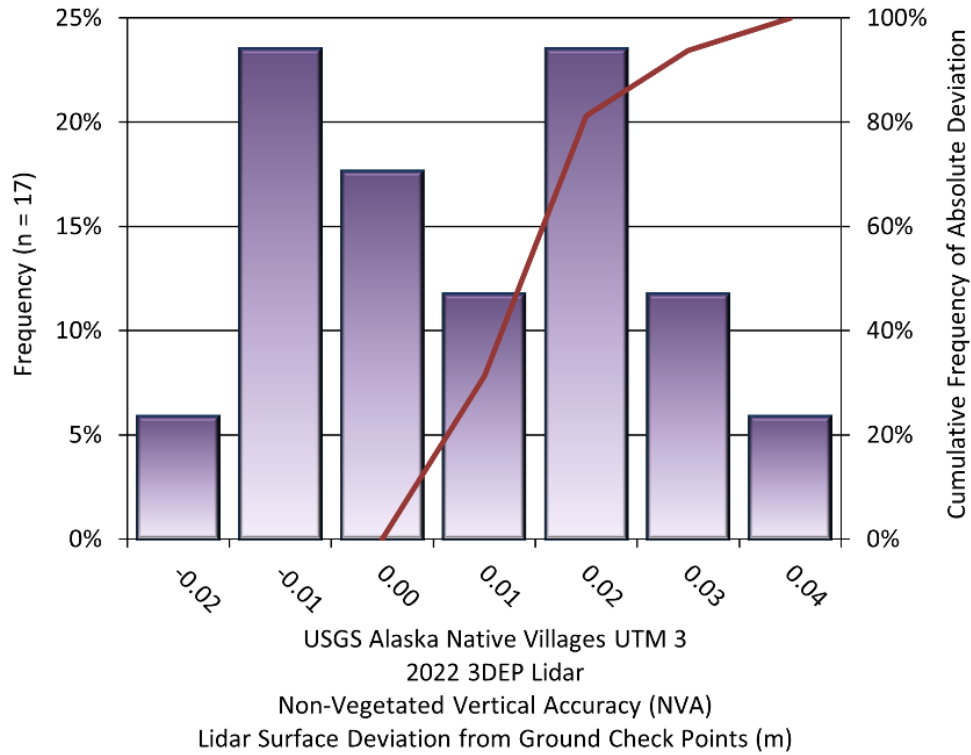


Figure 18: Frequency histogram for the lidar classified LAS deviation from ground check point values (NVA) for the zone UTM 3

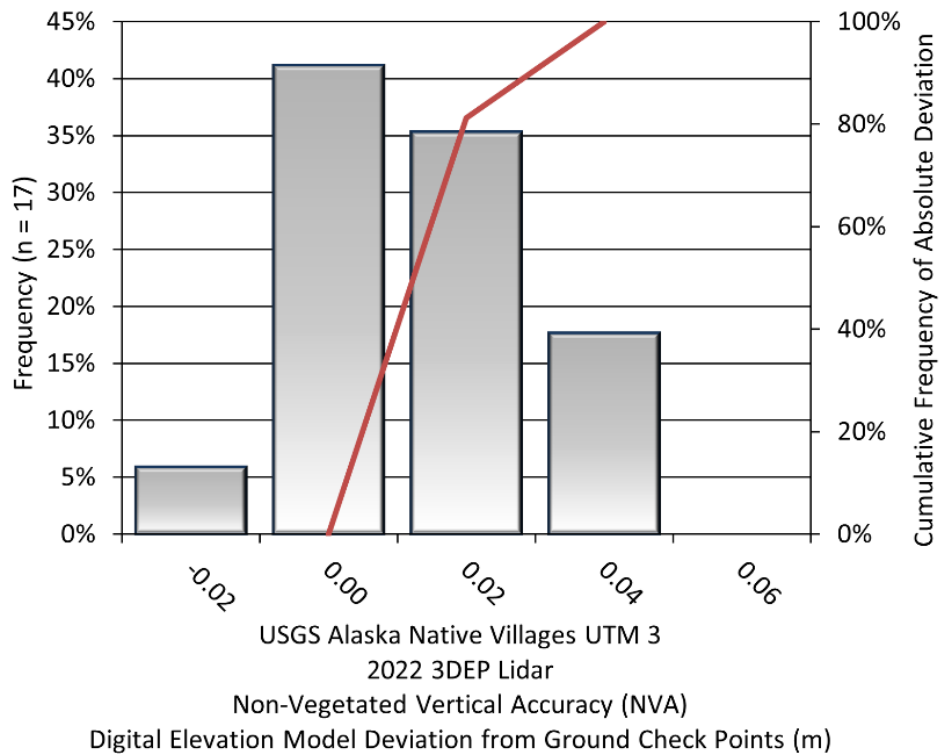


Figure 19: Frequency histogram for the lidar bare earth DEM surface deviation from ground check point values (NVA) for the zone UTM 3

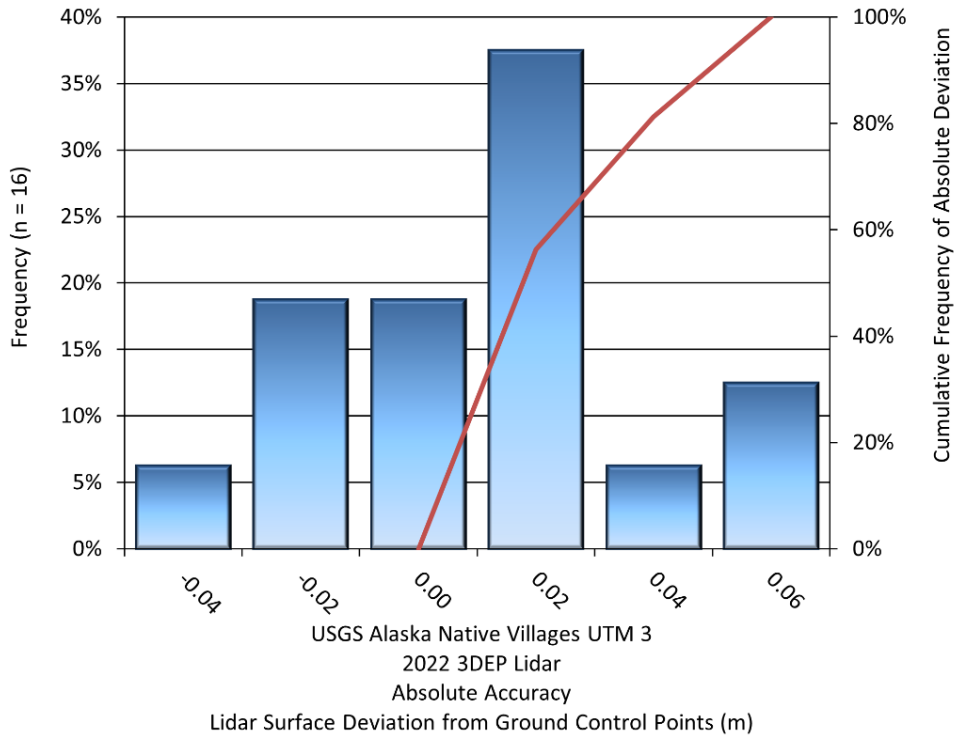


Figure 20: Frequency histogram for the lidar surface deviation from ground control point values for the zone UTM 3

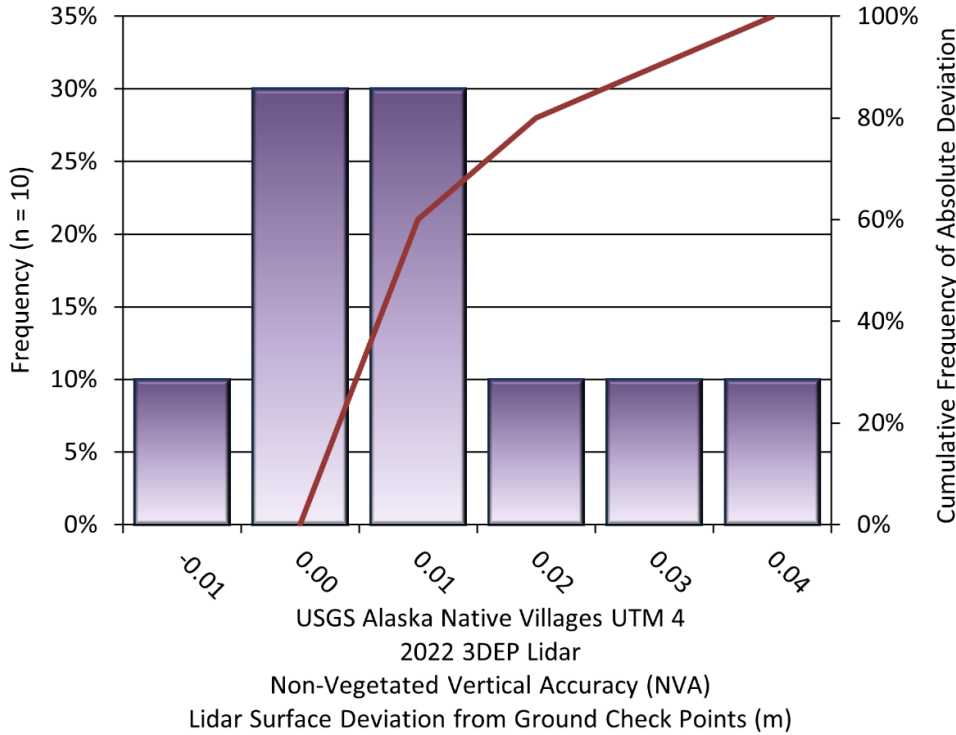


Figure 21: Frequency histogram for the lidar classified LAS deviation from ground check point values (NVA) for the zone UTM 4

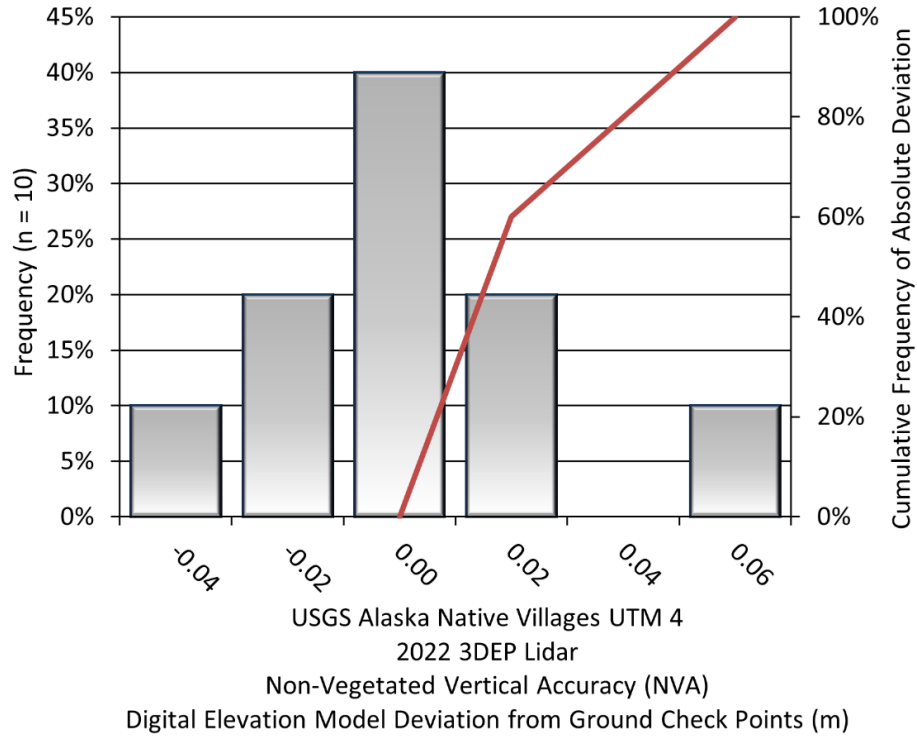


Figure 22: Frequency histogram for the lidar bare earth DEM surface deviation from ground check point values (NVA) for the zone UTM 4

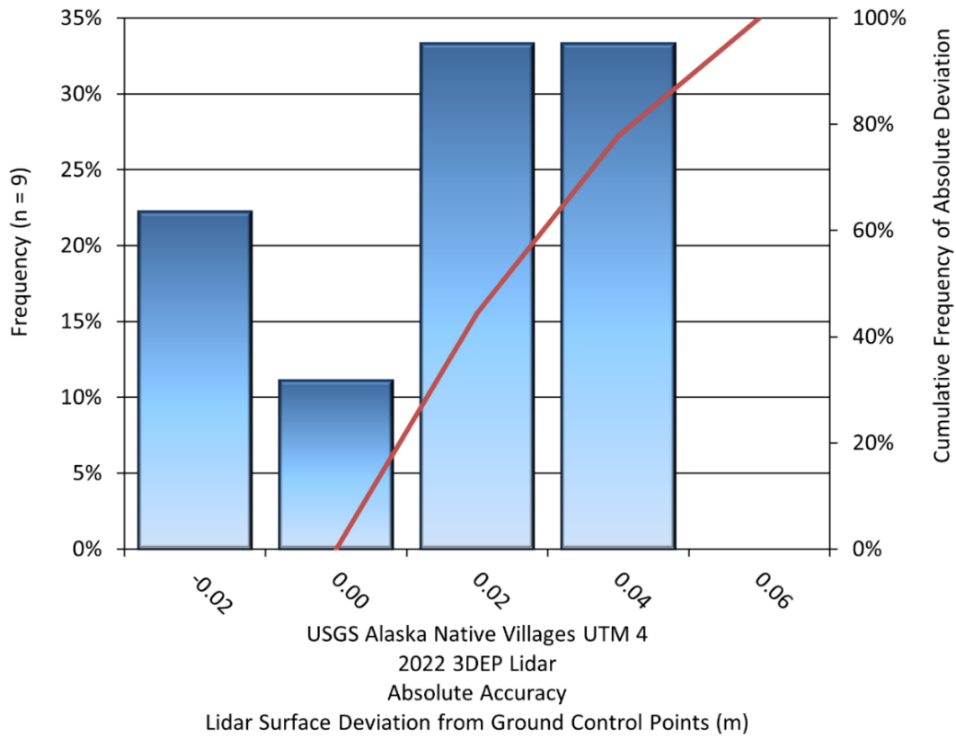


Figure 23: Frequency histogram for the lidar surface deviation from ground control point values for the zone UTM 4

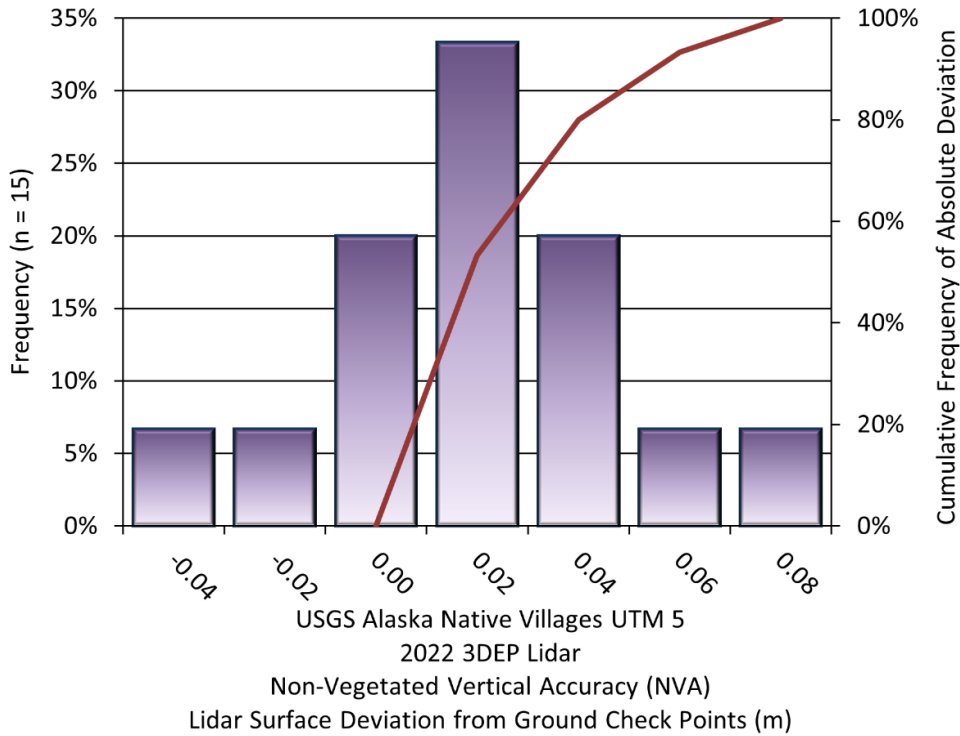


Figure 24: Frequency histogram for the lidar classified LAS deviation from ground check point values (NVA) for the zone UTM 5

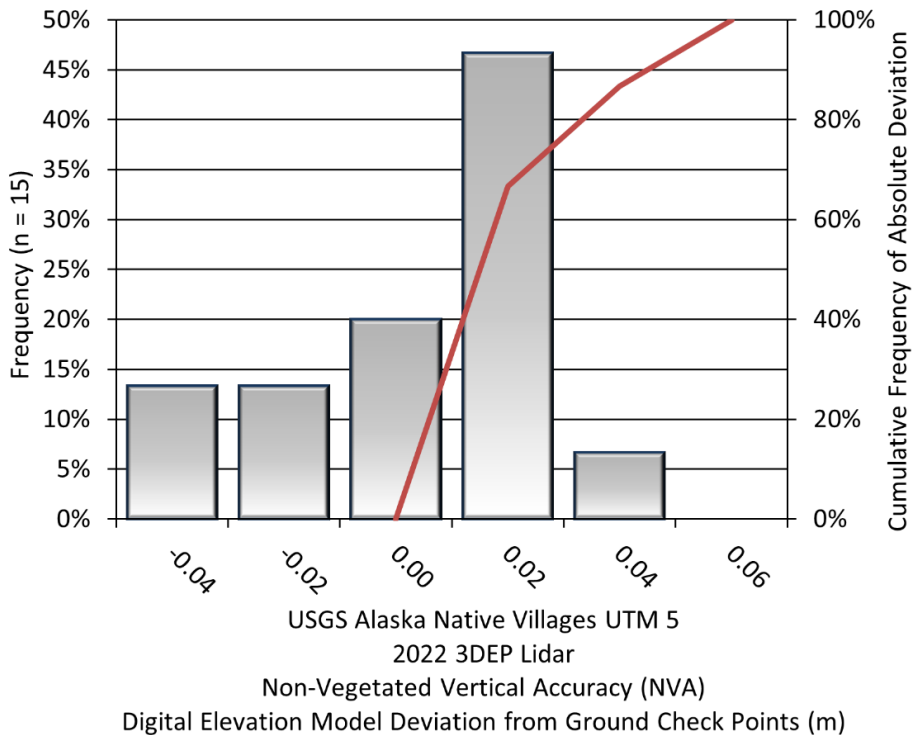


Figure 25: Frequency histogram for the lidar bare earth DEM surface deviation from ground check point values (NVA) for the zone UTM 5

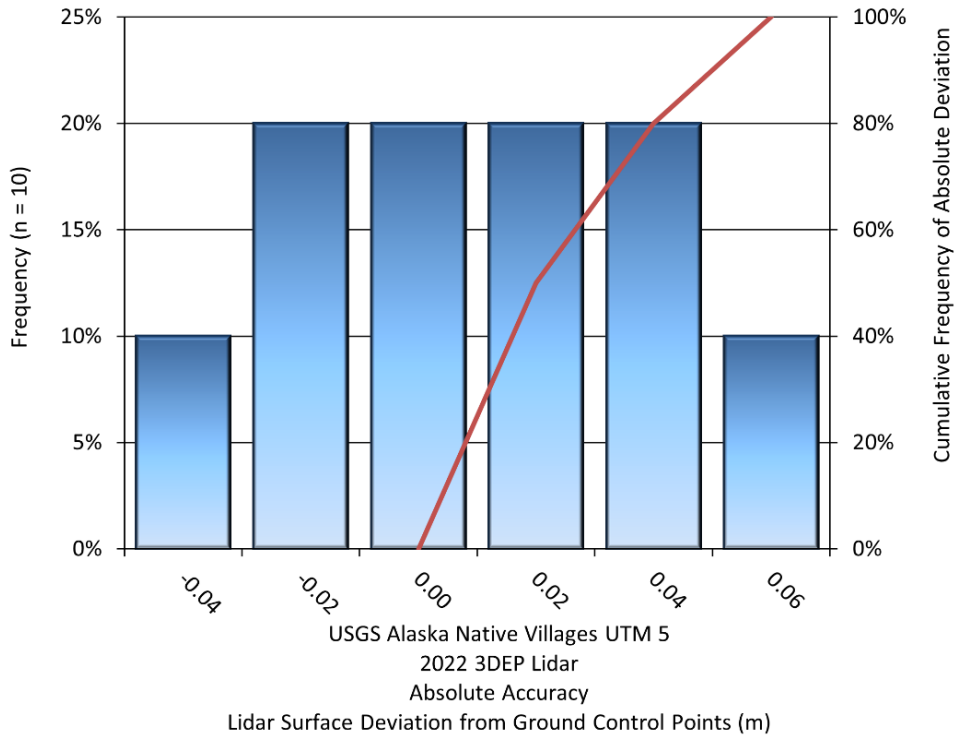


Figure 26: Frequency histogram for the lidar surface deviation from ground control point values for the zone UTM 5

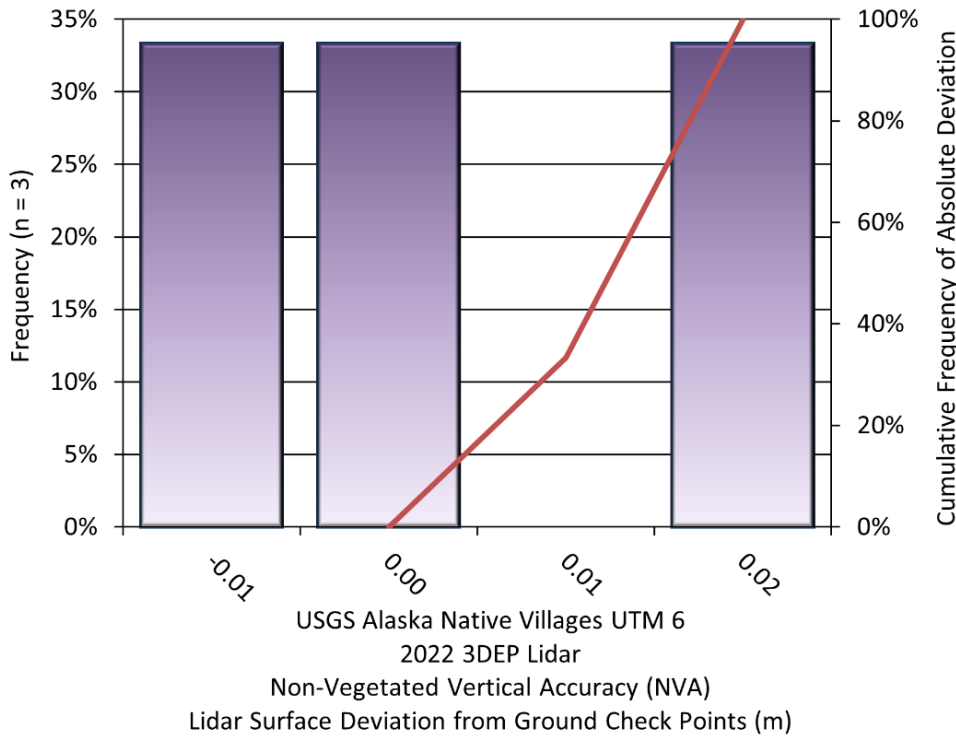


Figure 27: Frequency histogram for the lidar classified LAS deviation from ground check point values (NVA) for the zone UTM 6

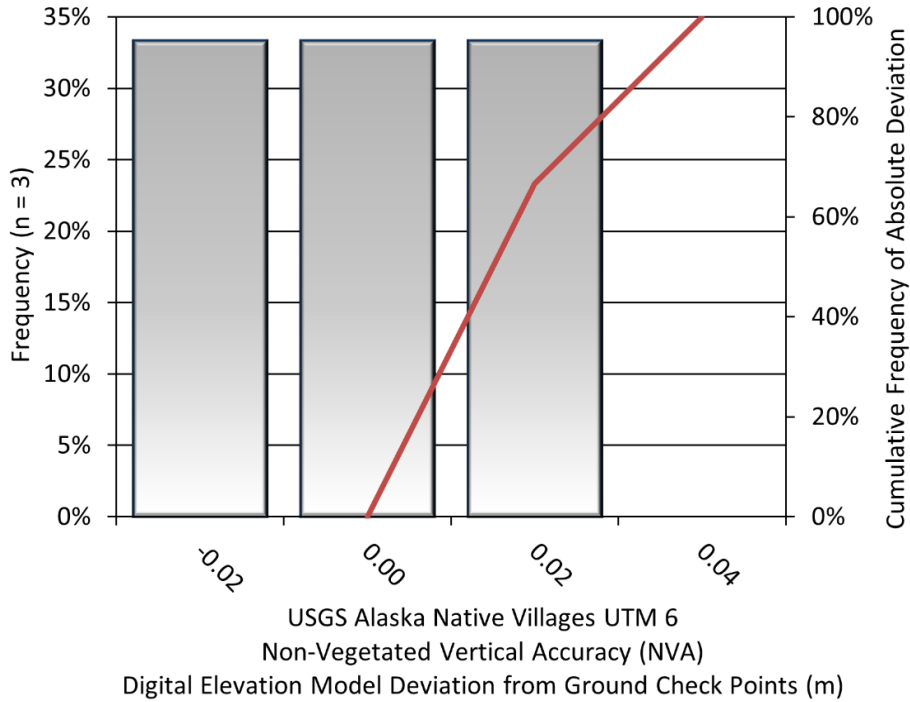


Figure 28: Frequency histogram for the lidar bare earth DEM surface deviation from ground check point values (NVA) for the zone UTM 6

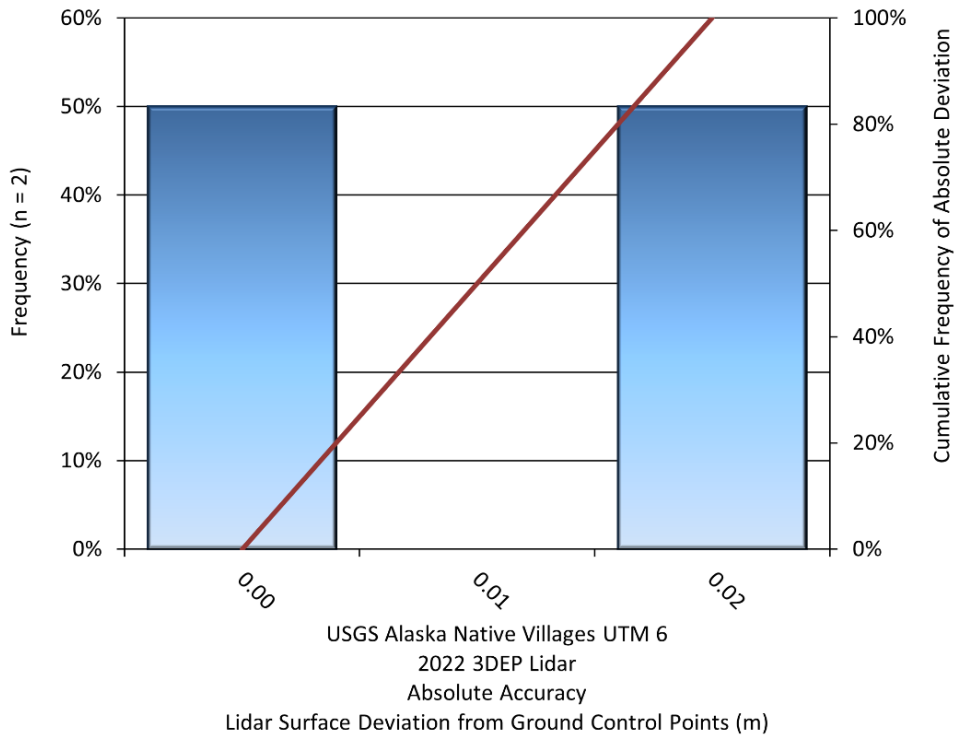


Figure 29: Frequency histogram for the lidar surface deviation from ground control point values for the zone UTM 6

Lidar Vegetated Vertical Accuracies

NV5 Geospatial also assessed vertical accuracy using Vegetated Vertical Accuracy (VVA) reporting. VVA compares known ground check point data collected over vegetated surfaces using land class descriptions to the triangulated ground surface generated by the ground classified lidar points. For the Native Villages survey, a total of 41 vegetated check points were collected and compared to the classified LAS (Table 13, Figure 30, Figure 32, Figure 34, and Figure 36) and bare earth DEM evaluated at the 95th percentile (Table 13, Figure 31, Figure 33, Figure 35, and Figure 37).

Table 13: Vegetated vertical accuracy results

UTM	Parameter	VVA, as compared to classified LAS	VVA, as compared to bare earth DEM
3	Sample	19 points	19 points
	95 th Percentile	0.239 m	0.258 m
	Average	0.089 m	0.084 m
	Median	0.087 m	0.103 m
	RMSE	0.131 m	0.130 m
	Standard Deviation (1 σ)	0.098 m	0.102 m
4	Sample	11 points	11 points
	95 th Percentile	0.276 m	0.260 m
	Average	0.156 m	-0.154 m
	Median	0.166 m	-0.153 m
	RMSE	0.185 m	0.177 m
	Standard Deviation (1 σ)	0.104 m	0.092 m
5	Sample	9 points	9 points
	95 th Percentile	0.280 m	0.291 m
	Average	0.126 m	-0.133 m
	Median	0.092 m	-0.082 m
	RMSE	0.157 m	0.166 m
	Standard Deviation (1 σ)	0.100 m	0.106 m
6	Sample	2 points	2 points
	95 th Percentile	0.143 m	0.129 m
	Average	0.088 m	-0.078 m
	Median	0.088 m	-0.078 m
	RMSE	0.107 m	0.096 m
	Standard Deviation (1 σ)	0.087 m	0.080 m

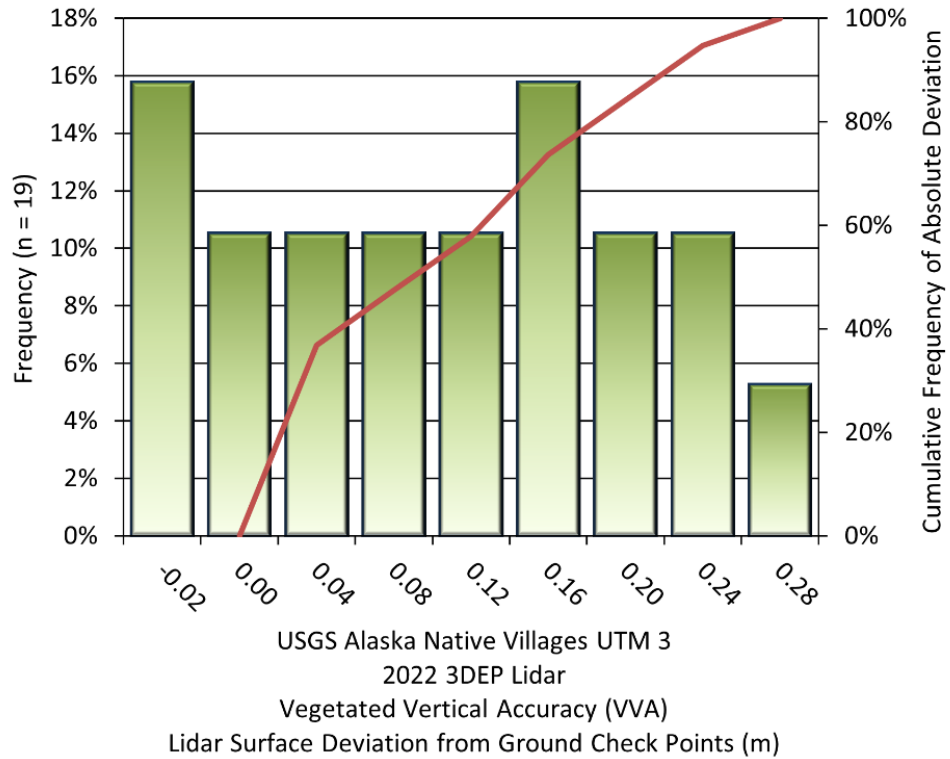


Figure 30: Frequency histogram for the lidar surface deviation from all land cover class point values (VVA) for the zone UTM 3

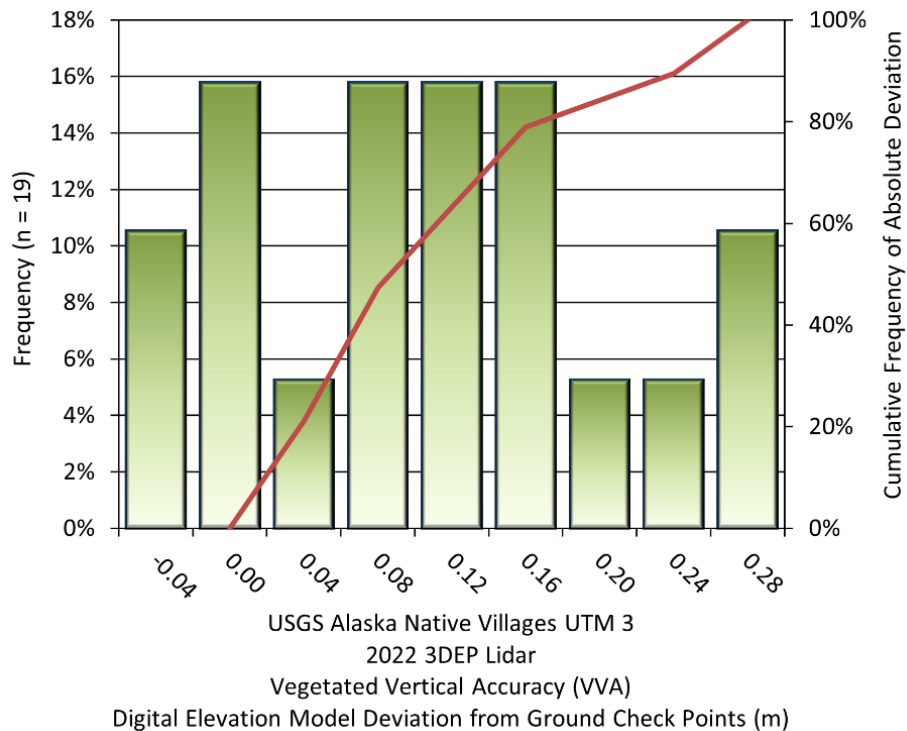


Figure 31: Frequency histogram for the lidar bare earth DEM deviation from vegetated check point values (VVA) for the zone UTM 3

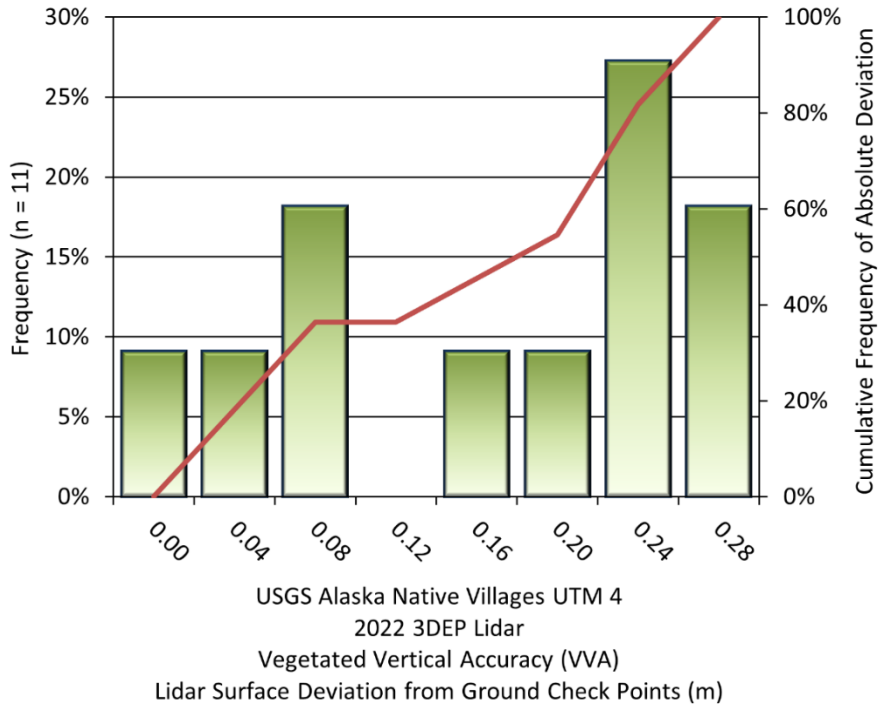


Figure 32 Frequency histogram for the lidar surface deviation from all land cover class point values (VVA) for the zone UTM 4

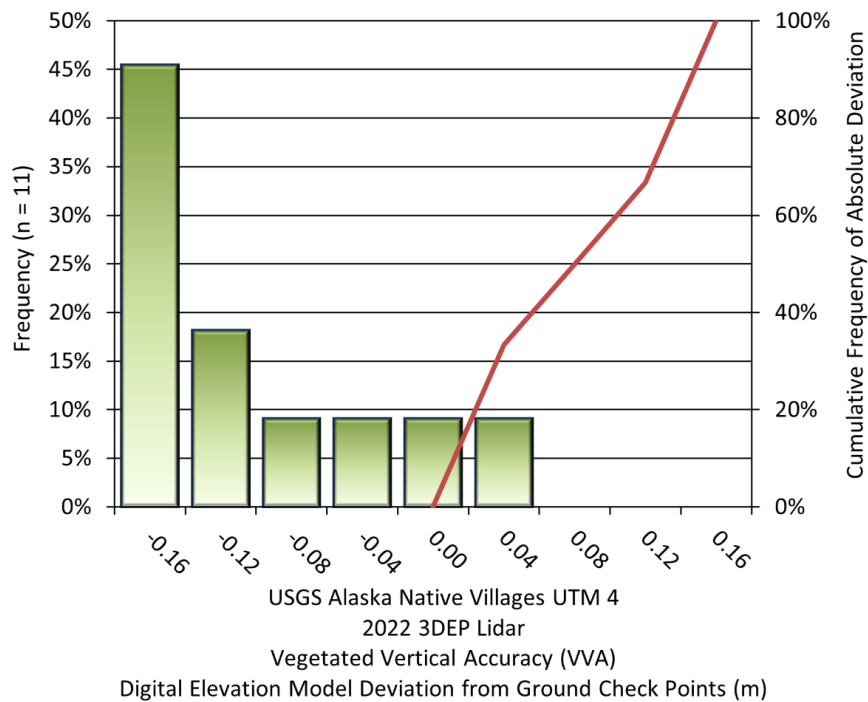


Figure 33: Frequency histogram for the lidar bare earth DEM deviation from vegetated check point values (VVA) for the zone UTM 4

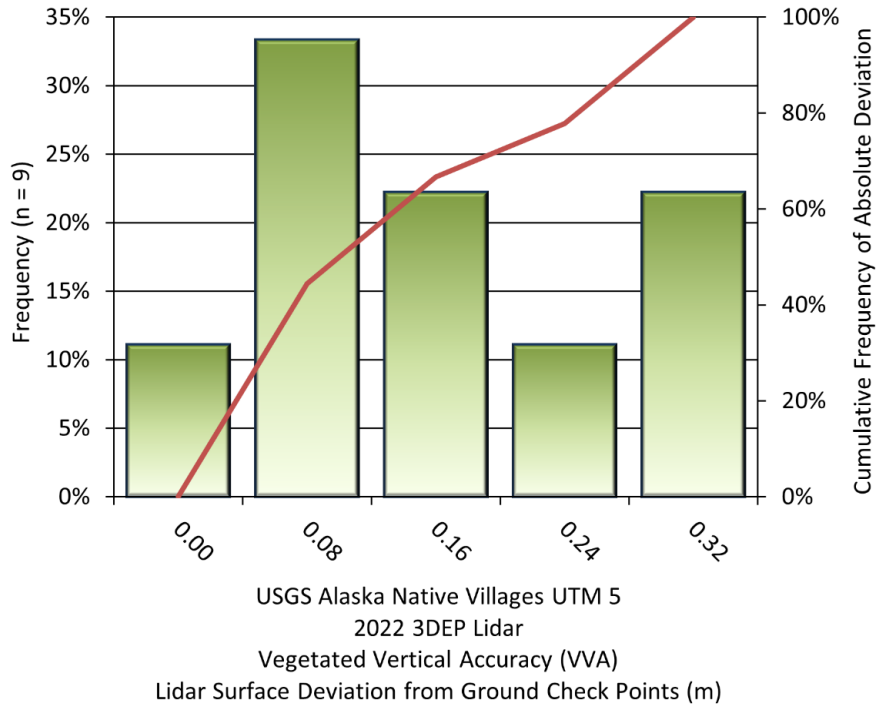


Figure 34: Frequency histogram for the lidar surface deviation from all land cover class point values (VVA) for the zone UTM 5

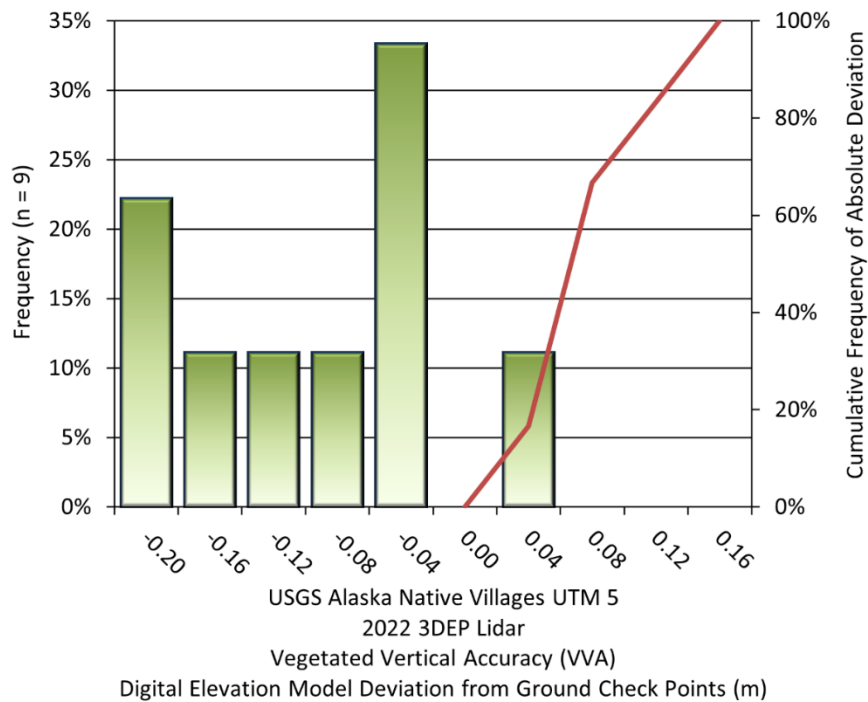


Figure 35: Frequency histogram for the lidar bare earth DEM deviation from vegetated check point values (VVA) for the zone UTM 5

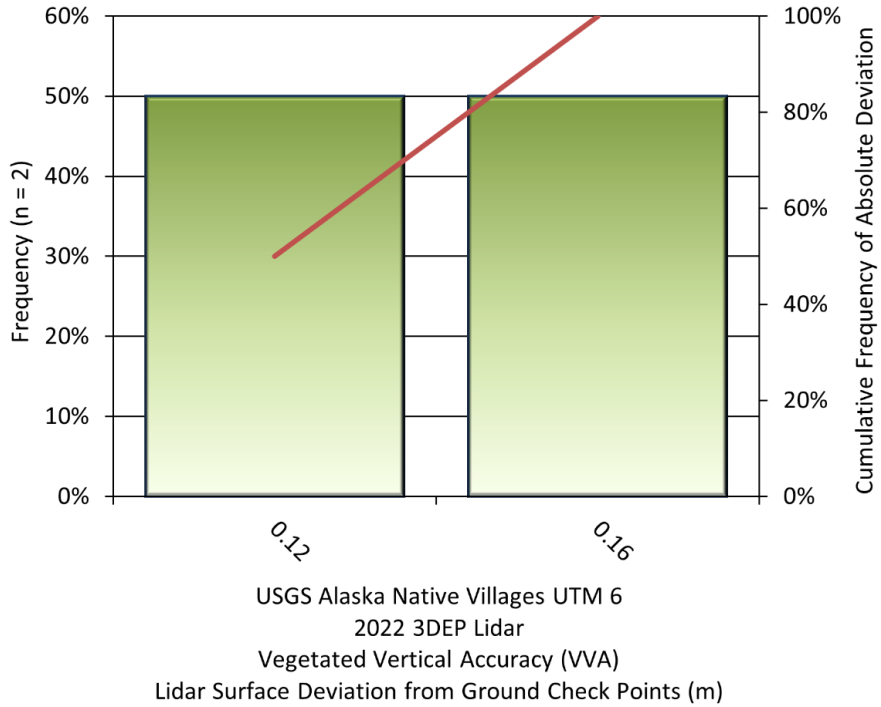


Figure 36: Frequency histogram for the lidar surface deviation from all land cover class point values (VVA) for the zone UTM 6

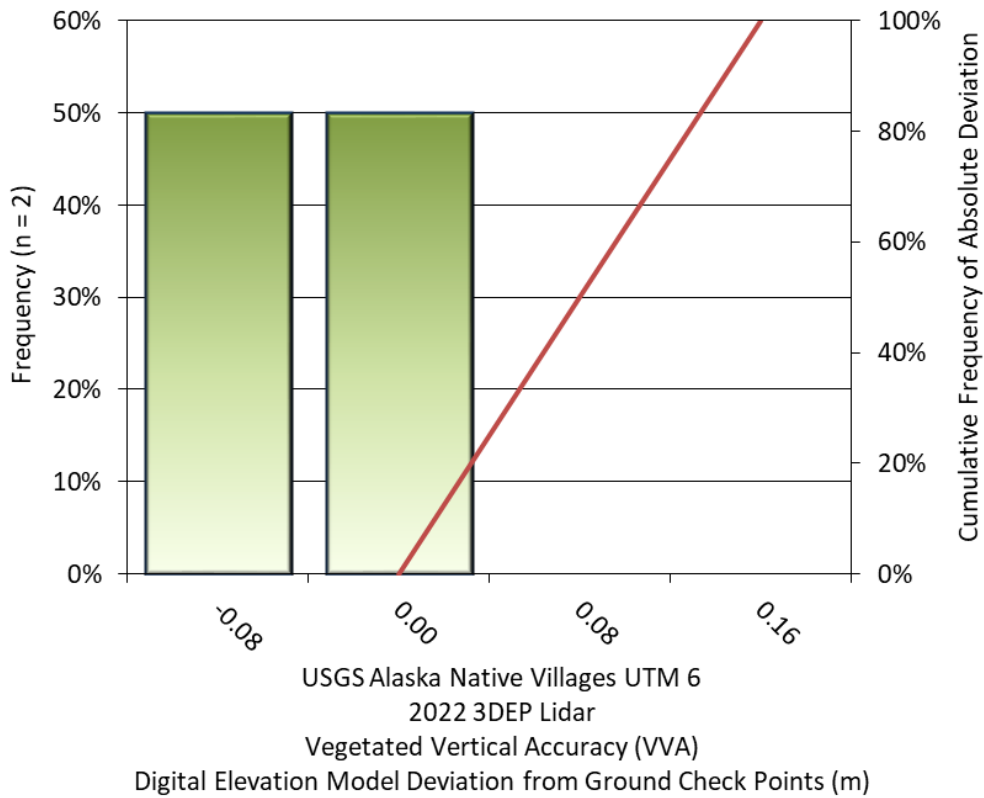


Figure 37: Frequency histogram for the lidar bare earth DEM deviation from vegetated check point values (VVA) for the zone UTM 6

Lidar Relative Vertical Accuracy

Relative vertical accuracy refers to the internal consistency of the data set as a whole: the ability to place an object in the same location given multiple flight lines, GPS conditions, and aircraft attitudes. When the lidar system is well calibrated, the swath-to-swath vertical divergence is low (<0.10 meters). The relative vertical accuracy was computed by comparing the ground surface model of each individual flight line with its neighbors in overlapping regions. The average relative accuracy is shown in Table 14 and Figure 38 through Figure 41.

Table 14: Relative accuracy results

UTM	Parameter	Relative Accuracy
3	Sample	18 surfaces
	Average	0.031 m
	Median	0.031 m
	RMSE	0.031 m
	Standard Deviation (1 σ)	0.003 m
	1.96 σ	0.005 m
4	Sample	9 surfaces
	Average	0.032 m
	Median	0.034 m
	RMSE	0.036 m
	Standard Deviation (1 σ)	0.006 m
	1.96 σ	0.012 m
5	Sample	13 surfaces
	Average	0.043 m
	Median	0.041 m
	RMSE	0.042 m
	Standard Deviation (1 σ)	0.003 m
	1.96 σ	0.006 m
6	Sample	5 surfaces
	Average	0.037 m
	Median	0.037 m
	RMSE	0.038 m
	Standard Deviation (1 σ)	0.001 m
	1.96 σ	0.002 m

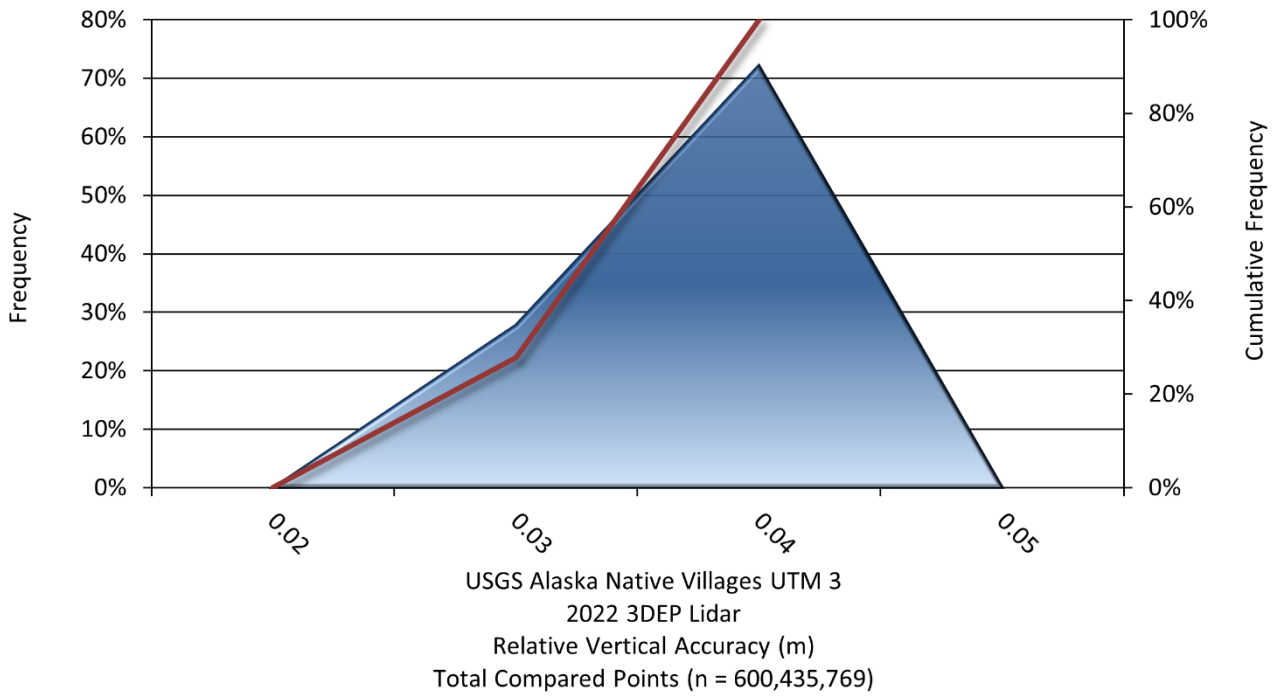


Figure 38: Frequency plot for the relative vertical accuracy between flight lines for UTM 3

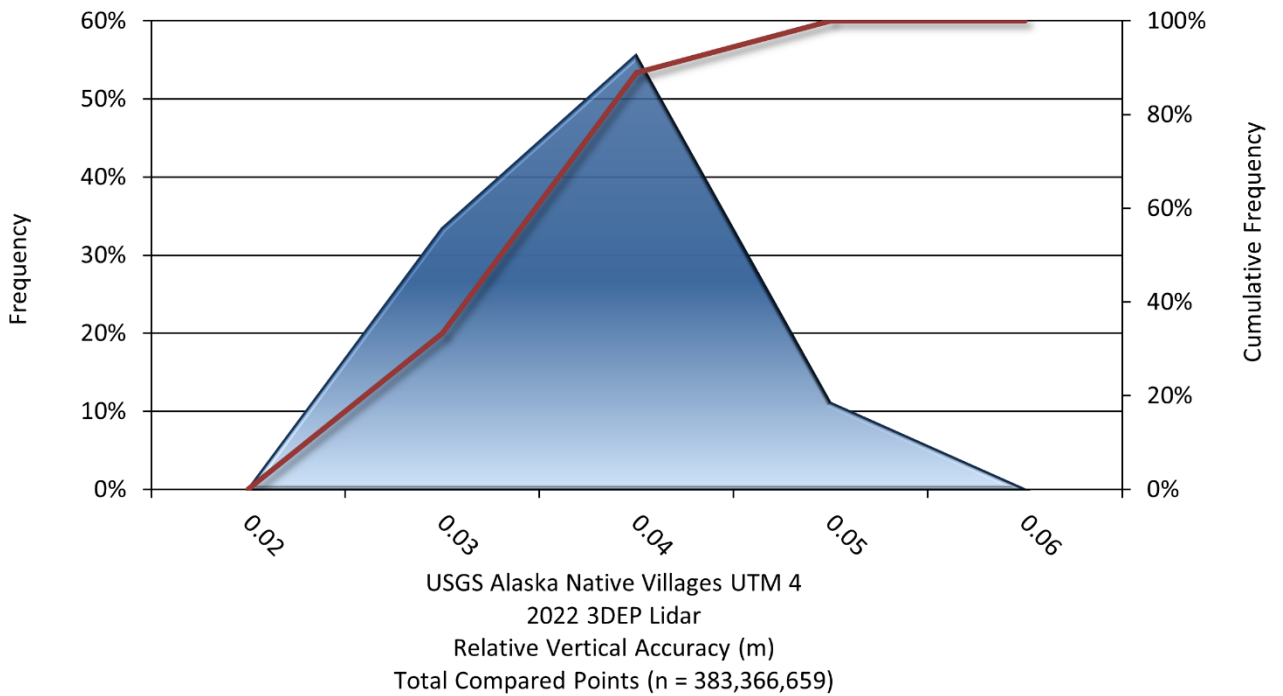


Figure 39: Frequency plot for the relative vertical accuracy between flight lines for UTM 4

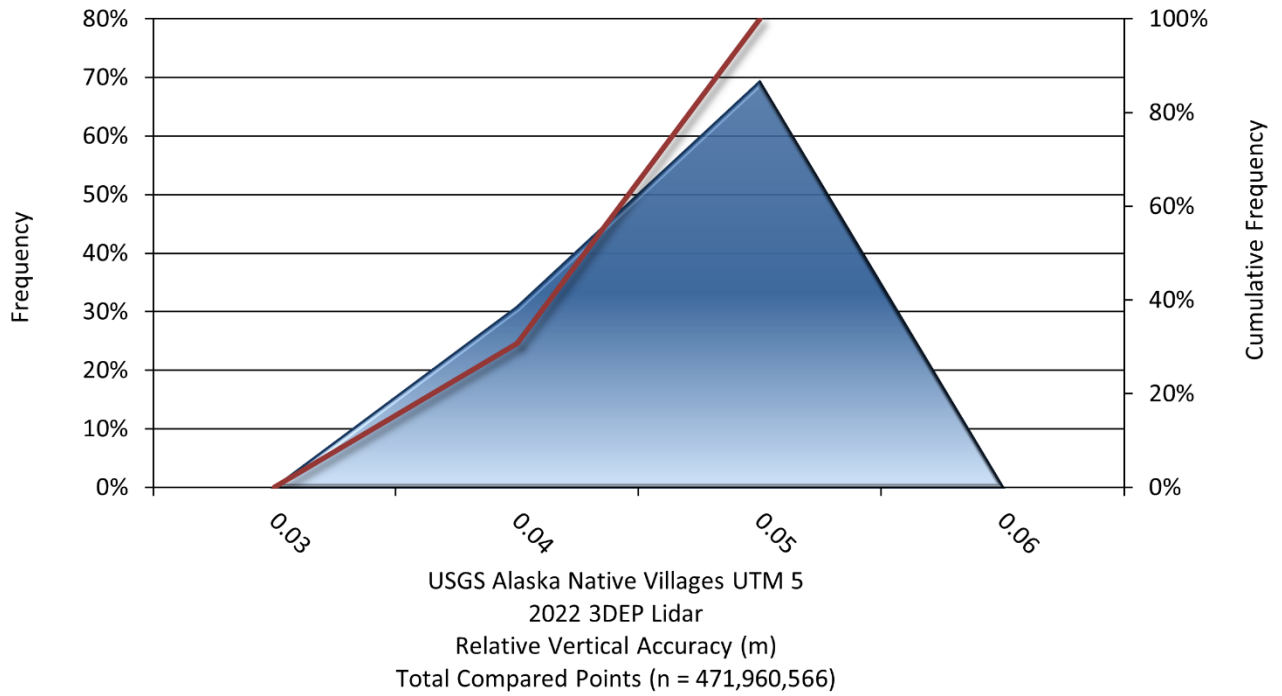


Figure 40: Frequency plot for the relative vertical accuracy between flight lines for UTM 5

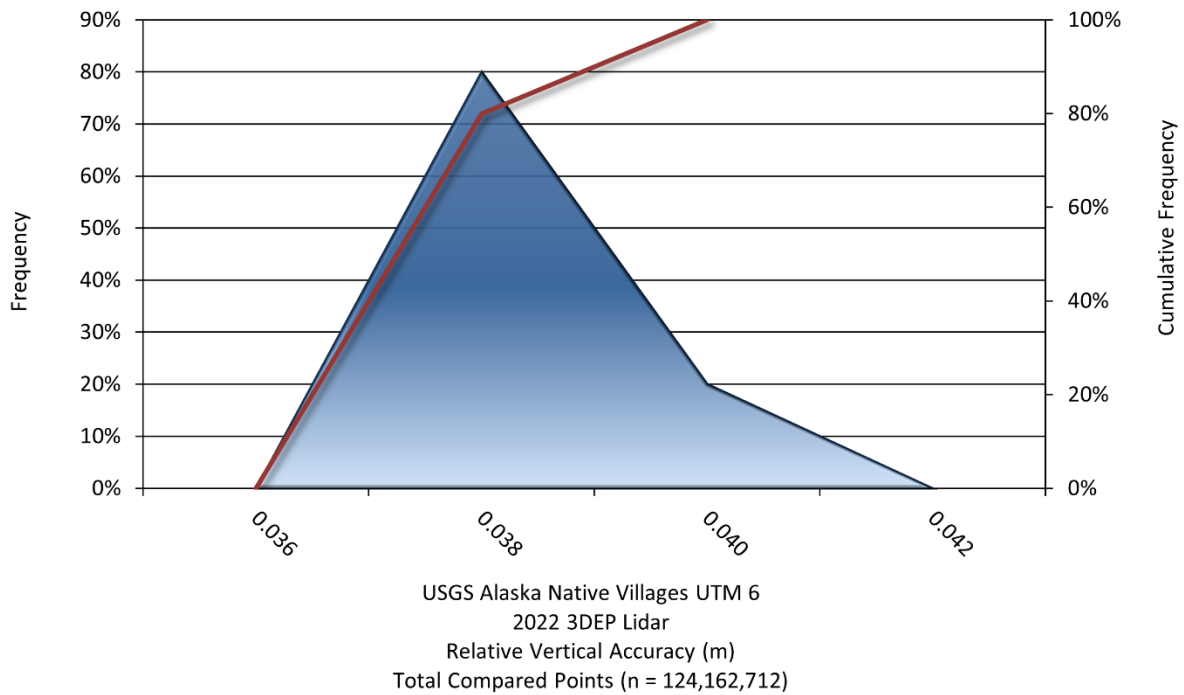


Figure 41: Frequency plot for the relative vertical accuracy between flight lines for UTM 6

Lidar Horizontal Accuracy

Lidar horizontal accuracy is a function of Global Navigation Satellite System (GNSS) derived positional error, flying altitude, and INS derived attitude error. The maximum GNSS positional error was derived from the laser trajectory using NV5’s proprietary LAS processing software, Las Monkey. The obtained $RMSE_r$ value is multiplied by a conversion factor of 1.7308 to yield the horizontal component of the National Standards for Spatial Data Accuracy (NSSDA) reporting standard where a theoretical point will fall within the obtained radius 95 percent of the time. All the villages in this project had a flying altitude of 2500 meters and a GNSS positional error of 0.023 meters. In addition to these parameters, the villages in the UTM 3 zone had an IMU error of 0.003 decimal degrees, which was produced to meet a 0.407 m horizontal accuracy at the 95% confidence level (Table 15). The rest of the villages had an IMU error of 0.002 and a horizontal accuracy of 0.273 m.

Table 15: Horizontal Accuracy

UTM	Parameter	Horizontal Accuracy
3	$RMSE_r$	0.235 m
	ACC_r	0.407 m
4	$RMSE_r$	0.158 m
	ACC_r	0.273 m
5	$RMSE_r$	0.158 m
	ACC_r	0.273 m
6	$RMSE_r$	0.158 m
	ACC_r	0.273 m

CERTIFICATIONS

NV5 Geospatial provided lidar services for the Native Villages project as described in this report.

I, Steven Miller, have reviewed the attached report for completeness and hereby state that it is a complete and accurate report of this project.



Jul 26, 2023

Steven Miller
Project Manager
NV5 Geospatial

I, Evon P. Silvia, PLS, being duly registered as a Professional Land Surveyor in and by the state of Alaska, hereby certify that the methodologies, static GNSS occupations used during airborne flights, and ground survey point collection were performed using commonly accepted Standard Practices. Field work conducted for this report was conducted by DOWL and under the supervision of their survey staff.

Accuracy statistics shown in the Accuracy Section of this Report have been reviewed by me and found to meet the "National Standard for Spatial Data Accuracy".



Jul 26, 2023

Evon P. Silvia, PLS
NV5 Geospatial
Corvallis, OR 97330



Signed: Jul 26, 2023

COA: 125659

GLOSSARY

1-sigma (σ) Absolute Deviation: Value for which the data are within one standard deviation (approximately 68th percentile) of a normally distributed data set.

1.96 * RMSE Absolute Deviation: Value for which the data are within two standard deviations (approximately 95th percentile) of a normally distributed data set, based on the FGDC standards for Non-vegetated Vertical Accuracy (NVA) reporting.

Accuracy: The statistical comparison between known (surveyed) points and laser points. Typically measured as the standard deviation (σ) and root mean square error (RMSE).

Absolute Accuracy: The vertical accuracy of lidar data is described as the mean and standard deviation (σ) of divergence of lidar point coordinates from ground survey point coordinates. To provide a sense of the model predictive power of the dataset, the root mean square error (RMSE) for vertical accuracy is also provided. These statistics assume the error distributions for x, y and z are normally distributed, and thus we also consider the skew and kurtosis of distributions when evaluating error statistics.

Relative Accuracy: Relative accuracy refers to the internal consistency of the data set; i.e., the ability to place a laser point in the same location over multiple flight lines, GPS conditions and aircraft attitudes. Affected by system attitude offsets, scale and GPS/IMU drift, internal consistency is measured as the divergence between points from different flight lines within an overlapping area. Divergence is most apparent when flight lines are opposing. When the lidar system is well calibrated, the line-to-line divergence is low (<10 cm).

Root Mean Square Error (RMSE): A statistic used to approximate the difference between real-world points and the lidar points. It is calculated by squaring all the values, then taking the average of the squares and taking the square root of the average.

Data Density: A common measure of lidar resolution, measured as points per square meter.

Digital Elevation Model (DEM): File or database made from surveyed points, containing elevation points over a contiguous area. Digital terrain models (DTM) and digital surface models (DSM) are types of DEMs. DTMs consist solely of the bare earth surface (ground points), while DSMs include information about all surfaces, including vegetation and man-made structures.

Intensity Values: The peak power ratio of the laser return to the emitted laser, calculated as a function of surface reflectivity.

Nadir: A single point or locus of points on the surface of the earth directly below a sensor as it progresses along its flight line.

Overlap: The area shared between flight lines, typically measured in percent. 100% overlap is essential to ensure complete coverage and reduce laser shadows.

Pulse Rate (PR): The rate at which laser pulses are emitted from the sensor; typically measured in thousands of pulses per second (kHz).

Pulse Returns: For every laser pulse emitted, the number of wave forms (i.e., echoes) reflected back to the sensor. Portions of the wave form that return first are the highest element in multi-tiered surfaces such as vegetation. Portions of the wave form that return last are the lowest element in multi-tiered surfaces.

Real-Time Kinematic (RTK) Survey: A type of surveying conducted with a GPS base station deployed over a known monument with a radio connection to a GPS rover. Both the base station and rover receive differential GPS data and the baseline correction is solved between the two. This type of ground survey is accurate to 1.5 cm or less.

Post-Processed Kinematic (PPK) Survey: GPS surveying is conducted with a GPS rover collecting concurrently with a GPS base station set up over a known monument. Differential corrections and precisions for the GNSS baselines are computed and applied after the fact during processing. This type of ground survey is accurate to 1.5 cm or less.

Scan Angle: The angle from nadir to the edge of the scan, measured in degrees. Laser point accuracy typically decreases as scan angles increase.

Native Lidar Density: The number of pulses emitted by the lidar system, commonly expressed as pulses per square meter.

APPENDIX A - ACCURACY CONTROLS

Relative Accuracy Calibration Methodology:

Manual System Calibration: Calibration procedures for each mission require solving geometric relationships that relate measured swath-to-swath deviations to misalignments of system attitude parameters. Corrected scale, pitch, roll and heading offsets were calculated and applied to resolve misalignments. The raw divergence between lines was computed after the manual calibration was completed and reported for each survey area.

Automated Attitude Calibration: All data were tested and calibrated using TerraMatch automated sampling routines. Ground points were classified for each individual flight line and used for line-to-line testing. System misalignment offsets (pitch, roll and heading) and scale were solved for each individual mission and applied to respective mission datasets. The data from each mission were then blended when imported together to form the entire area of interest.

Automated Z Calibration: Ground points per line were used to calculate the vertical divergence between lines caused by vertical GPS drift. Automated Z calibration was the final step employed for relative accuracy calibration.

Lidar accuracy error sources and solutions:

Source	Type	Post Processing Solution
Long Base Lines	GPS	None
Poor Satellite Constellation	GPS	None
Poor Antenna Visibility	GPS	Reduce Visibility Mask
Poor System Calibration	System	Recalibrate IMU and sensor offsets/settings
Inaccurate System	System	None
Poor Laser Timing	Laser Noise	None
Poor Laser Reception	Laser Noise	None
Poor Laser Power	Laser Noise	None
Irregular Laser Shape	Laser Noise	None

Operational measures taken to improve relative accuracy:

Low Flight Altitude: Terrain following was employed to maintain a constant above ground level (AGL). Laser horizontal errors are a function of flight altitude above ground (about 1/3000th AGL flight altitude).

Focus Laser Power at narrow beam footprint: A laser return must be received by the system above a power threshold to accurately record a measurement. The strength of the laser return (i.e., intensity) is a function of laser emission power, laser footprint, flight altitude and the reflectivity of the target. While surface reflectivity cannot be controlled, laser power can be increased and low flight altitudes can be maintained.

Reduced Scan Angle: Edge-of-scan data can become inaccurate. The scan angle was reduced to a maximum of $\pm 29.25^\circ$ from nadir, creating a narrow swath width and greatly reducing laser shadows from trees and buildings.

Quality GPS: Flights took place during optimal GPS conditions (e.g., 6 or more satellites and PDOP [Position Dilution of Precision] less than 3.0). Before each flight, the PDOP was determined for the survey day. During all flight times, a dual frequency DGPS base station recording at 1 second epochs was utilized and a maximum baseline length between the aircraft and the control points was less than 13 nm at all times.

Ground Survey: Ground survey point accuracy (<1.5 cm RMSE) occurs during optimal PDOP ranges and targets a minimal baseline distance of 4 miles between GPS rover and base. Robust statistics are, in part, a function of sample size (n) and distribution. Ground survey points are distributed to the extent possible throughout multiple flight lines and across the survey area.

Opposing Flight Lines: All overlapping flight lines have opposing directions. Pitch, roll and heading errors are amplified by a factor of two relative to the adjacent flight line(s), making misalignments easier to detect and resolve.